

# Fock space localization in the Sachdev-Ye-Kitaev model

F. Monteiro, T. Micklitz

*Centro Brasileiro de Pesquisas Físicas, Rua Xavier Sigaud 150, 22290-180, Rio de Janeiro, Brazil*

Masaki Tezuka

*Department of Physics, Kyoto University, Kyoto 606-8502, Japan*

Alexander Altland

*Institut für Theoretische Physik, Universität zu Köln, Zùlpicher Str. 77, 50937 Cologne, Germany*

(Dated: April 18, 2022)

We study the physics of many body localization in the Majorana Sachdev-Ye-Kitaev (SYK) model perturbed by a one-body Hamiltonian. Specifically, we consider the statistics of many body wave functions and spectra as the strength of the one-body term is ramped up from an ergodic phase via a regime of non-ergodic yet extended states into a (Fock space) Anderson localized phase. Our results are obtained from an effective low energy theory, derived from the microscopic model by matrix integral techniques standard in the theory of disordered electronic systems. Applicable to systems of arbitrarily large particle number, the analytical results produced by this formalism are compared to exact diagonalization for systems containing up to 30 Majorana fermions. The statistics of many body spectra and wave functions, and the indications of the localization transition are in quantitative agreement with numerics. We believe that this is the first many body system where a localization transition is observed in parameter free agreement with first principle analytical calculations.

PACS numbers: 05.45.Mt, 72.15.Rn, 71.30.+h

## I. INTRODUCTION

Quantum mechanical wave functions in random environments often show non-ergodic or ‘localized’ behavior. Half a century after the first discovery in Ref. 1, we now distinguish three universality classes: (i) *Anderson localization* (AL) of single particle wave functions, (ii) *Fock space localization* (FSL) in the many particle Fock spaces of interacting but spatially confined quantum systems [2–6], and (iii) *many body localization* (MBL) in spatially extended geometries [7, 8]. While Anderson localization is now relatively well understood, the situation in the interacting cases is less clear. The degree of uncertainty shows in that even the principal manifestations of MBL in extended geometries remain controversial [9–12]. Many body localization is a tough problem for it combines the complexity of strong interactions with that of spatial extendedness. The explosion of Fock space dimensions as the number of degrees of freedom increases makes numerical access to the phenomenon infamously hard. In this regard, the phenomenon of Fock space localization occupies an interesting middle ground: driven by correlations, it is in a universality class different from Anderson localization. However, absent spatial extension, the localizing and delocalizing tendencies of interactions are more transparent than in traditional MBL settings.

Starting with the seminal paper [2], key aspects of FSL have been addressed in numerous studies [4, 13–22]. The most striking signature distinguishing FSL from AL is that the passage between ergodic and localized states in Fock spaces occurs via an intermediate regime where states remain extended but with non-uniform distribution. At this point, the nature of this

regime of *non-ergodic extended states* (NEE states) is only partially understood. Absent both first principle descriptions and sufficiently high powered numerics of genuinely interacting systems, the NEE regime is described in terms of model systems mimicking the complexity of Fock spaces, such as Bethe lattices [17, 23], or random regular graphs [16, 17, 21, 24]. However, even there, the situation remains somewhat opaque, some authors predicting NEE regimes with (multi)fractal many body wave function statistics [17], and others [25, 26] less drastic scenarios of reduced Hilbert space wave function support.

In this paper, we discuss FSL for a genuinely interacting fermionic quantum system, the SYK model. The SYK Hamiltonian has become a model paradigm for strongly correlated quantum matter [27–33]. Generalized for the presence of a one-body contribution, its complex version describes spatially confined correlated quantum matter as quantum dots, heavy nuclei, or complex molecules. We here focus on the real (Majorana) variant, where the lack of number conservation makes for a somewhat simpler description at essentially unaltered FSL properties. The point made in this paper is that the system is amenable to analytic solution by first principle methods of localization theory [34, 35]. For all we know, this is the only many body system which can be described from first principles all the way from ergodic regimes, over an intermediate regime of non-ergodic extended states into the phase of strong Fock space localization.

Topics addressed below include:

- the diagnostics of the FSL transition via spectral statistics,

- the description of the NEE regime via many body wave function statistics,
- the analytical identification of the FSL localization transition, and
- comparison of these results to exact diagonalization data obtained for systems of size  $N = 11, 13, 15$ , where the SYK model is in the unitary symmetry class A. (While our results do not depend qualitatively on the system's symmetry, the numerical factors entering a parameter free comparison do, and we focus on the class A setting for simplicity.)

To some degree, the work reported here builds on a previous publication [36], where three of the present authors demonstrated the existence of a regime of non-ergodic extended states for a simpler random energy variant of the SYK model which, however, does not correspond to a 'realistic' few body Hamiltonian.

*Model:* the SYK Hamiltonian [37, 38]

$$\hat{H}_4 = \frac{1}{4!} \sum_{i,j,k,l=1}^{2N} J_{ijkl} \hat{\chi}_i \hat{\chi}_j \hat{\chi}_k \hat{\chi}_l, \quad (1)$$

describes a system of  $2N$  Majorana fermions,  $\{\hat{\chi}_i, \hat{\chi}_j\} = 2\delta_{ij}$ , subject to an all-to-all interaction, with matrix elements  $\{J_{ijkl}\}$  drawn from a Gaussian distribution of variance  $\langle |J_{ijkl}|^2 \rangle = 6J_4^2/(2N)^3$ . Defined in this way, it defines an ideal of a massively interacting quantum system lacking any degree of internal structure. Due to the 'least information' principle realized through the stochastic interaction, all single particle orbitals,  $i$ , stand on equal footing, and the absence of a continuous  $U(1)$ -symmetry prevents the fragmentation of the Fock space into sectors of conserved particle number. Reflecting these features, the physics of the SYK Hamiltonian at large time scales becomes equivalent to that of random matrix theory (RMT), with wave functions homogeneously distributed over the full Hilbert space.

A tendency to Fock space localization is included by adding to  $\hat{H}_4$  a free particle contribution [39, 40],

$$\hat{H}_2 = \frac{1}{2} \sum_{j,k=1}^{2N} J_{ij} \hat{\chi}_i \hat{\chi}_j, \quad (2)$$

with a likewise random antisymmetric matrix  $J_{ij} = -J_{ji}$ , with matrix elements  $\{J_{ij}\}$  drawn from a Gaussian of variance  $\langle |J_{ij}|^2 \rangle = J_2^2/2N$ .

We now discuss in what sense  $\hat{H}_2$  induces localization. Without loss of generality, we may assume  $\{J_{ij}\}$  to be diagonalized into a form  $\hat{H}_2 = i \sum_i^N v_i \hat{\chi}_{2i-1} \hat{\chi}_{2i}$ , where  $\pm v_i$  are the eigenvalues of the hermitian matrix  $i\{J_{ij}\}$ . We define  $N$  complex fermion annihilation operators  $\hat{c}_i = \frac{1}{2}(\hat{\chi}_{2i-1} + i\hat{\chi}_{2i})$  for  $i = 1, \dots, N$ , satisfying  $\{\hat{c}_i, \hat{c}_j^\dagger\} = \delta_{ij}$ , and number operators  $\hat{n}_i = \hat{c}_i^\dagger \hat{c}_i$ , and  $\hat{H}_2$  assumes the

form

$$\hat{H}_2 = \sum_{i=1}^N v_i (2\hat{n}_i - 1). \quad (3)$$

This shows that for asymptotically strong  $\hat{H}_2$  the Fock space eigenstates are localized in the  $2^N$  states of the Fermion occupation number basis,  $|n\rangle = |n_1, n_2, \dots, n_N\rangle$ ,  $n_i = 0, 1$ . Seen in this way, the Fock space becomes a hypercube defined by the  $2^N$  corner sites  $|n\rangle = |0, 0, 1, 0, 0, 1, 0\rangle$ ,  $\hat{H}_2$  defines an on-site localizing potential, and  $\hat{H}_4$  a hopping operator connecting sites of maximal bit separation 4. (For two states  $|n\rangle, |m\rangle$  we define the Hamming distance  $|n - m|$  as the number of bits in which the states differ. The action of the hopping operator is limited to states of Hamming distance four and less.) [41] The nature of the ensuing random lattice system is illustrated in Fig. 1 for a Fock space of 14 Majorana fermions. The figure indicates the connectivity of the state  $|0001100\rangle$  to illustrate the characteristics of the lattice structure — sparsity, irregularity of connections, and statistical correlation of random hopping amplitudes due to the small number of independent random coefficients in an exponentially high dimensional space.

*Plan of the paper:* In view of the somewhat technical core parts of our analysis, section II contains a qualitative discussion of the physics of the system and a summary of all our results. In section III we map the computation of disorder averaged correlation functions onto that of an equivalent matrix integral. In section IV, a stationary phase approach is applied to reduce the matrix integral to an effective theory describing physics at large time scales. In sections V and VI we apply this representation to the discussion of wave function statistics and the localization transition, respectively. We conclude in section VII. Technical parts of our analysis are relegated to a number of Appendices.

## II. SUMMARY OF RESULTS

The intuitive picture behind FSL in the SYK system is similar to that of many body localization in spatially extended systems. For asymptotically strong  $\hat{H}_2$ , states are localized in  $|n\rangle$  with associated Poisson correlated eigenvalues [42]  $v_n \equiv \sum_i v_i (2n_i - 1)$ . The interaction Hamiltonian  $\hat{H}_4$  induces hopping via transitions  $|n\rangle \rightarrow |m\rangle$ . Expressing  $\hat{H}_4$  in terms of complex Fermion creation and annihilation operators, we see that  $|n\rangle$  and  $|m\rangle$  differ at most by four in their total occupation number  $n \equiv \sum_i n_i$ . Although  $\hat{H}_4$  contains only an algebraically small number  $\sim N^4 \sim \log(D)$  of independent matrix elements, it is efficient at inducing many body chaos, including for strengths of  $\hat{H}_2$  much larger than those of  $\hat{H}_4$ . To see how, assume that the typical eigenvalues of  $\hat{H}_2$  are distributed over a range of width  $\Delta$ . According to the central limit theorem, this implies that the individual  $v_i$  are

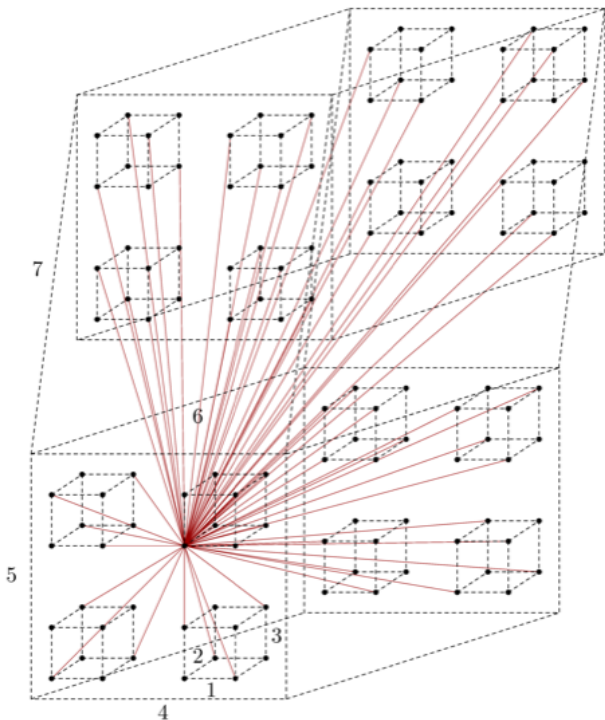


FIG. 1: Hypercubic Fock space of an  $2N = 14$  Majorana system. The numbers indicate the bit depth of states in the computational fermion basis, and the lines are a qualitative representation of the connectivity of the reference state  $|0001100\rangle$ . For large values of  $N$ , the pattern of connections becomes sparse. However, there remain exponentially many  $\propto D$  connections, statistically correlated due to the small number of  $\sim N^4$  of independent random amplitudes.

distributed over a width

$$\delta \equiv \Delta/N^{1/2}. \quad (4)$$

For convenience, we scale the distribution width  $J_4 \equiv J = (2/N)^{1/2}$  and  $J_2 = \delta$ , such that the SYK<sub>4</sub> band width  $w_4 = \sqrt{J_4^2 N/2}$  equals unity, and the SYK<sub>2</sub> band width  $w_2 = \sqrt{J_2^2 N} = \Delta$ . [43]

#### A. Four regimes with different localization behavior

In the following, we will show that four regimes of different disorder strength need to be distinguished:

- I:  $\delta < N^{-1/2}$ : On-site disorder lesser than the SYK<sub>4</sub> band width — ergodic regime.
- II:  $N^{-1/2} < \delta \ll 1$ : On-site disorder exceeding SYK<sub>4</sub> band width, but differences in energy between sites connected by  $\hat{H}_4$  smaller than it.
- III:  $1 < \delta < N^2$ : Site-to-site variations stronger than SYK<sub>4</sub> band width.

IV:  $N^2 < \delta$  Fock space localization.

The regimes of smallest and highest on site disorder, I and IV, respectively, are the easiest to understand: in I the band width of the diagonal is lesser than that of the SYK<sub>4</sub> Hamiltonian. Wave functions are ergodic, and the spectral statistics is of Wigner-Dyson type, as in the unperturbed case. In the complementary regime IV, wave functions are localized on individual Fock space sites  $n$  with energies  $v_n$ . Such sites may hybridize with neighbors  $m$  of energy  $v_m$  if the energies are resonant with the strength of the coupling matrix element,  $J/N^{3/2} \sim |v_n - v_m|$  [7]. Typical nearest neighbor energy differences are of  $\mathcal{O}(\delta)$ , but there is also a large number  $\sim N^4$  of them. The expected number of resonant neighbors thus scales as  $N^4 \frac{J}{N^{3/2}\delta}$  which equals  $N^2/\delta$  for our chosen units. This leads to the heuristic criterion  $\delta \sim N^2$  for delocalization, confirmed (up to corrections logarithmic in  $N$ ) by the analysis below.

For energies between the extremes,  $N^{-1/2} < \delta < N^2$ , wave functions are neither localized nor ergodically extended. A key quantity to the description of these regimes is the local SYK<sub>4</sub> averaged band center spectral density,  $\nu_n \equiv -\frac{1}{\pi} \text{Im} \langle \langle n | (0^+ - \hat{H}_2 - \hat{H}_4)^{-1} | n \rangle \rangle_J$ , where  $\langle \dots \rangle_J$  stands for averaging over realizations of  $H_4$ . Below, we show that this quantity is given by

$$\begin{aligned} \nu_n &= \frac{1}{\pi} \text{Im} \frac{1}{v_n - i\kappa_n}, \\ \kappa_n &\equiv \pi (\mathcal{P}\hat{\nu})_n \equiv \pi \sum_m \mathcal{P}_{|n-m|} \nu_m, \end{aligned} \quad (5)$$

where the first line states that the average local density of states (DoS) is defined by states broadened by a scale  $\kappa_n$ , and the second line expresses the broadening as a sum over SYK<sub>4</sub> hybridization processes governed by the nearest neighbor energy denominators  $\pi\nu_m$  and a hopping operator  $\mathcal{P}$ . The latter is unit normalized as  $\sum_m \mathcal{P}_{|n-m|} = 1$  and limited to state separations  $|n-m| \leq 4$  (see Eq. (28) for the precise definition), while  $\hat{\nu}$  (here and in the following) denotes a diagonal matrix in occupation basis with diagonal elements  $\nu_n$ . Eq. (5) is a self consistent equation for the local density of states,  $\nu_n$ , and the level hybridization,  $\kappa_n$ . What simplifies its solution is the effectively random distribution of site energies,  $v_m$ , affecting the DoS at  $n$ . The largeness  $\mathcal{O}(N^4)$  of these contributions justifies a statistical approach, which leads to the solution

$$\begin{aligned} \kappa_n &\simeq \kappa \Theta(C - |v_n|), \\ (\kappa, C) &= \begin{cases} (1, 1), & \delta < 1 \quad (\text{I, II}), \\ (\delta^{-1}, \delta), & \delta > 1 \quad (\text{III, IV}). \end{cases} \end{aligned} \quad (6)$$

This result states that (for center energy  $E = 0$ ) only sites with energy lower than a threshold  $C$  contribute to the DoS. The value of this threshold depends on the spread of the site energy spectrum, where in the weak disorder regimes, I, II, sites within the SYK<sub>4</sub> band width all contribute,  $C = 1$ , and the levels are broadened over

the full band width. For stronger disorder, III, IV, the spectral support is limited to energies  $|v_n| < \delta$ . With  $v_n$  distributed over a range  $\sim N^{1/2}\delta$ , the ratio of *active sites* to the total number of sites is  $\sim N^{-1/2}$ , which depends on  $N$  but not on the energy spreading itself. Within this restricted set, there is a still smaller set of energies  $|v_n| \lesssim \delta^{-1} \sim \kappa_n$  defining a class of *resonant sites* for which the real part of the energy denominator,  $v_n$ , is comparable to the broadening,  $\kappa$ . This hierarchy makes regime III different from II where all active sites are automatically resonant. Active and resonant sites define the support of many body wave functions in regimes I-III. However, to describe how this materializes in concrete ways, we need information beyond the average spectral density.

In the rest of the paper, we consider the spectral two point correlation function at the band center

$$K(\omega) \equiv \frac{1}{\nu^2} \langle \nu(\frac{\omega}{2}) \nu(-\frac{\omega}{2}) \rangle_c, \quad (7)$$

and the moments of wave functions  $|\psi\rangle$  of zero energy,  $\epsilon_\psi$ ,

$$I_q \equiv \frac{1}{\nu} \sum_n \langle |\langle \psi | n \rangle|^{2q} \delta(\epsilon_\psi) \rangle_J, \quad (8)$$

as principal diagnostic quantities. In these expressions,  $\nu = \nu(E \simeq 0)$ ,  $\nu(E) = \sum_\psi \langle \delta(E - \epsilon_\psi) \rangle_J$  is the SYK<sub>4</sub> averaged many body density of states at zero energy  $E \simeq 0$  and the subscript  $c$  refers to the connected correlation function,  $\langle \nu(\frac{\omega}{2}) \nu(-\frac{\omega}{2}) \rangle_J - \langle \nu(\frac{\omega}{2}) \rangle_J \langle \nu(-\frac{\omega}{2}) \rangle_J$ .

## B. Spectral statistics

In regimes I-III wave functions are extended and their eigenenergies are correlated, with Wigner-Dyson statistics. Assuming an odd number  $N$  of complex fermions (for which the SYK model is in the unitary symmetry class A), this reflects in the spectral statistics of the Gaussian unitary ensemble (GUE),

$$\tilde{K}(s) = 1 - \frac{\sin^2 s}{s^2} + \delta(s/\pi), \quad s = \pi\omega\nu, \quad (9)$$

where  $\nu = \sum_n \nu_n$  is the average density of states. Differences between the regimes I-III show in the value of this scale, which in essence counts the number of active sites according to Eq. (6). To obtain a more explicit expression, we assume that the summation over  $n$  sites can be replaced by an average over the distribution of site energies,  $v_n$ . This leads to

$$\nu \equiv \sum_n \nu_n = cD \begin{cases} 1 & \text{I,} \\ \frac{1}{\sqrt{N}\delta} & \text{II, III,} \end{cases} \quad (10)$$

where, here and throughout,  $c = \mathcal{O}(1)$  represents numerical constants, and

$$D = 2^{N-1} \quad (11)$$

is the dimension of Fock space projected onto sites of definite (even, for concreteness) occupation number parity. (Both  $\hat{H}_{4,2}$  conserve parity and we focus on a definite parity sector.) The second line of Eq. (10) states that in the regimes of intermediate disorder strength, only a fraction  $D/\sqrt{N}\delta$  of active sites contributes to the spectral support of wave functions.

## C. Wave function statistics

In the weak disorder regime, I, wave functions are ergodically distributed over the full Fock space, with moments given by those of the Porter-Thomas distribution,

$$I_q = q! D^{1-q}, \quad \text{I,} \quad (12)$$

otherwise found for the wave functions of random matrix Hamiltonians. The result states that the complex amplitudes  $\langle n | \psi \rangle$  are independently distributed Gaussian random variables.

In regimes II and above the wave functions no longer ergodically occupy the full Fock space. The bulk of their support is concentrated on the subset of resonant sites. This behavior reflects in the moments

$$I_q = c^q \left( \frac{D}{\sqrt{N}\delta} \right)^{1-q} \frac{2q(2q-3)!!}{\kappa^{q-1}}, \quad \text{II, III,} \quad (13)$$

where  $c = \mathcal{O}(1)$ . To make the connection of this expression to Eq. (12) more transparent, consider the case of large  $q$ , where

$$q \gg 1: \quad I_q = cq! D_{\text{res}}^{1-q}, \quad (14)$$

$$D_{\text{res}} = D \begin{cases} \frac{1}{\sqrt{N}\delta} & \text{II,} \\ \frac{1}{\sqrt{N}\delta^2} & \text{III.} \end{cases}$$

These moments again coincide with those of a Gaussian distribution, now defined on the diminished number  $D_{\text{res}}$  of resonant sites in Fock space, over which the wave functions are uniformly spread. Noting that  $\delta \sim N^\alpha$ ,  $\alpha < 2$ , the dependence of  $D_{\text{res}}$  on  $D$  is approximated as

$$D_{\text{res}} = D / \log D^\beta, \quad \beta = \begin{cases} \alpha + 1/2 & \text{II,} \\ 2\alpha + 1/2 & \text{III.} \end{cases} \quad (15)$$

This suggests an interpretation in terms of a *weak fractal* whose dimension differs from the naive dimension by a factor  $D / \log D^\beta \sim D/D^0$ , rather than a strong fractal  $D/D^\gamma$  with some  $\gamma > 0$ .

Figures 2 and 3 show a comparison of our analytical predictions for the wave function moments dependence on  $\delta$  (Fig. 2), respectively  $q$  and  $N$  (Fig. 3), to numerical simulations for  $2N = 22, 26, 30$  Majorana fermions. Vertical dashed lines in Fig. 2 mark the boundaries between different regimes, and  $\delta_c$  is the scale at which Fock space localization sets in, see Eq. (43) and the refined expression, Eq. (F3), accounting for  $1/N$  corrections. For the numerically accessible  $N$ -values, regime II,

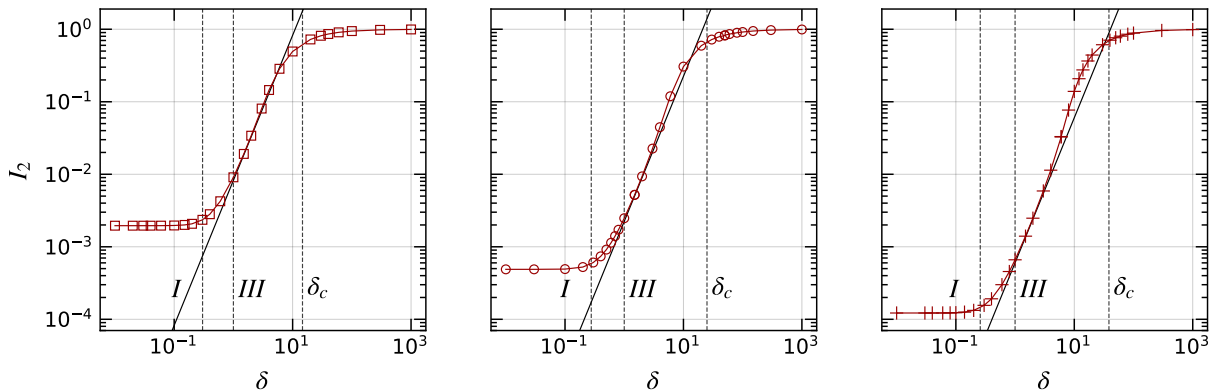


FIG. 2: Comparison of numerical computation of inverse participation ratio  $I_2$  as a function of the disorder strength  $\delta$  for system sizes  $N = 11$  (left),  $13$  (middle), and  $15$  (right) with the analytical prediction  $I_2 = 8\sqrt{N}\delta^2/(\pi D)$ , see Eq. (E8). Vertical dashed lines mark the end of region I, beginning of region III, and the scale  $\delta_c$  at which Fock space localization sets in (estimated from Eq. (F3)) [44].

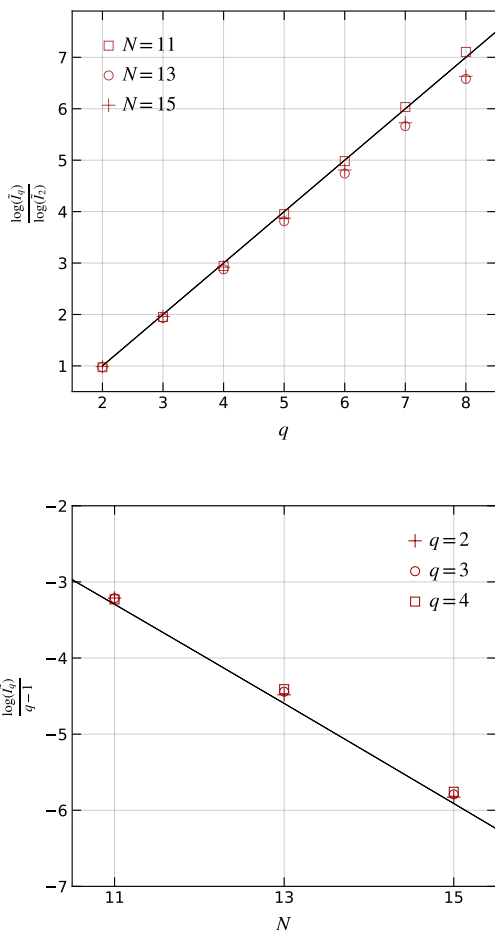


FIG. 3: Verification of the scaling of our analytical prediction Eq. (13) in  $q$  and  $N$ , respectively. In both panels we consider  $\delta = 3$  deep in regime III and  $\tilde{I}_q \equiv I_q/[q(2q-3)!!] = (4\sqrt{N}\delta^2/\pi D)^{q-1}$ , where the constants are taken from the accurate result for  $I_q$  in regime III, Eq. (E8).

$N^{-1/2} \ll \delta \ll 1$ , lacks the width required for the comparison with power laws and we concentrate on regime III. Given that there is no fitting of numerical parameters and numerical error bars are smaller than symbol size, the comparison is good. We notice a slight deviation in the  $q$ -scaling, increasing for large moments,  $q$ . However, this mismatch does not show consistent system size dependence, and cannot attribute a clear trend to it. Starting from  $N = 13$  we also see deviations of the predicted  $\delta$ -scaling at large values, which is a first indication of the proximity of the Anderson transition. At first sight, it may seem paradoxical that these signatures are first seen for larger  $N$ , where the parametric dependence of the localization threshold  $\delta \gtrsim N^2$  increases in  $N$ . However, the situation becomes clearer when we represent the inverse participation data as a function of a scaled parameter, as we will discuss next.

#### D. Strong localization

The wave functions describing random hopping on a lattice are localized on small sized clusters if, statistically, the nearest neighbor hopping matrix elements become smaller than the variations of the local site energies. For large  $N \gg 1$  this happens in our model for site disorder exceeding the localization threshold (43), where the logarithmic correction relative to the naive estimate  $\delta_c \sim N^2$  mentioned in the introduction accounts for resonant hybridization with sites beyond nearest neighbors [2]. However, in the real world of small sized systems  $N = \mathcal{O}(10)$  things are not as straightforward.

We first note that the result Eq. (43) is subject to both weak parametric corrections in  $N$ , and corrections in overall numerical factors. As for the former, the consistency equations describing the phase transition actually afford a solution in terms of the Lambert  $W$  function, Eq. (F3), which only for large  $N$  asymptotes to (43).

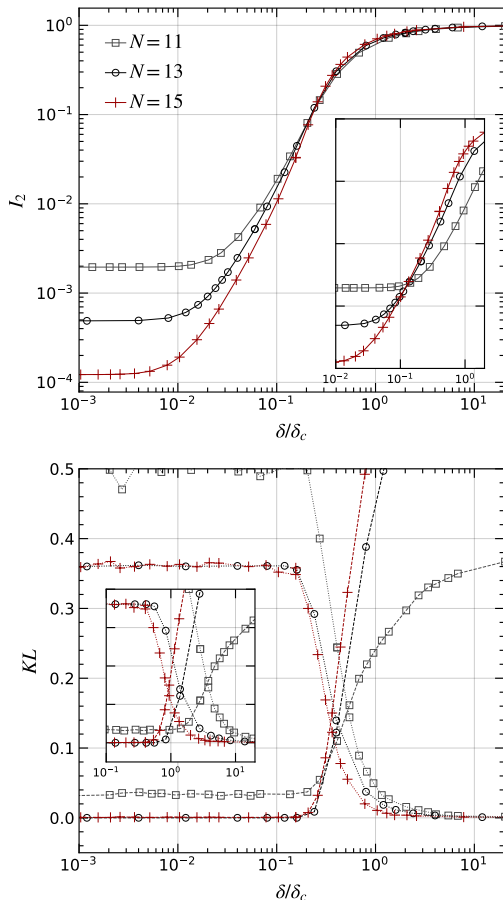


FIG. 4: Top: Scaling of the inverse participation ratio  $I_2$  for system sizes  $N = 11, 13, 15$  as functions of the dimensionless disorder strength  $\delta/\delta_c$ , where  $\delta_c$  is the critical strength obtained by analytical solution of the model in Eq. (F3). Bottom: plot of the relative Kullback-Leibler entropies  $KL$  between the numerical spectral statistics and the Wigner-Dyson (dashed) and Poisson distribution (dotted), respectively, for the same set of system sizes. In either case, the analytically obtained  $\delta_c$  overestimates the critical strength by an  $N$ -independent factor of  $\mathcal{O}(1)$ . Insets: Scaling of  $I_2$  and  $KL$  as functions of  $\delta/\delta_c$ , employing Eq. (43) with two adjusted numerical parameters, see discussion in main text.

On top of that, there are various sources for numerical deviations due to model approximations relying on the asymptotic largeness of parameters which in reality are finite.

Numerically, we detect the onset of localization via two indicators. The first is the wave function statistics, where  $I_2$  serves as a transition order parameter jumping between the values  $I_2 \sim D^{-1}$  in the ergodic weak disorder regime to  $I_2 \sim 1$  in the localized phase. Here, the first value must be taken with a grain of salt, again due to finite system size. Our discussion in the previous section shows that before reaching the transition, in regimes II, III, we have deviations away from the ergodic limit  $I_2 \sim D$ . In the thermodynamic limit, these are

inessential (because  $D$  is exponential in  $N$  while the corrections of Eq. (14) are in powers of  $N$ .) However, for system sizes in numerical reach, we cannot expect an actual jump in the order parameter. The best one can hope for is gradual steepening of the curve  $I_2(\delta)$  for  $\delta \rightarrow \delta_c$  upon increasing system size.

The second diagnostic is spectral statistics, Wigner-Dyson in the ergodic phase, Poisson in the localized phase. In the literature [45], the difference between the two types of statistics is often monitored by analysis of  $r$ -ratios [46], i.e. numerical comparison of the ratios  $r_k \equiv \frac{e_{k+1} - e_k}{e_k - e_{k-1}}$  between nearest neighbor many body energy levels,  $e_k$ , with the expected ratios for Poisson and Wigner-Dyson statistics. However, we have observed that naked eye comparisons can easily trick one into premature and qualitatively wrong conclusions. Instead, we adopt a more sophisticated entropic procedure detailed in Sec. VC and compute Kullback-Leibler divergences, where the latter are defined as relative entropies of the numerically observed distribution to the Poisson and Wigner-Dyson distribution, respectively.

Ideally, one would hope that both signatures, inverse participation ratio and spectral statistics reveal a phase transition via a crossing point when subjected to appropriate finite size scaling, and that that these crossing points sit at the same value. In reality, we almost, but not fully observe this behavior. In Fig. 4, we show the inverse participation ratio  $I_2$ , and the Kullback-Leibler entropy as a function of the scaled variable,  $\delta/\delta_c$ , where  $\delta_c$  is given by the analytical prediction Eq. (F3) in terms of the Lambert  $W$ -function. We observe that (i) both observables show reasonably well defined crossings with a tendency of sharpening behavior for increasing system size, however, (ii) these crossings deviate from the analytically predicted value  $\delta/\delta_c = 1$  by a numerical factor of  $\mathcal{O}(1)$ , and by a factor of similar magnitude among themselves. Turning to different scaling variables, one may sharpen the finite size scaling of either one of the two observables. For example, the inset in the first panel shows  $I_2$  as a function of  $\delta/\delta_c$ , with  $\delta_c$  from Eq. (43) with two numerical parameters outside and inside the ‘log’ adjusted to improve visibility of the crossing point [47]. However, this comes at the expense of a more diffuse scaling of the entropy, as shown in the inset of the second panel. We observe that the numerically obtained scaling for small systems responds sensitively to the finite  $N$  corrections (Eq. (F3) vs. Eq. (43)).

All in all, we consider the agreement with the numerics quite favorable. We see clear evidence of critical behavior in two observables and the position of the transition is obtained without free fit parameters from the analytical solution of an effective lattice model. This may be the first genuine Fock space localization problem where a first principle solution of this kind has been possible.

While the detailed analytical computations leading to Eq. (F3) are involved, their strategy, and the underlying approximations can be described in simple words. Our starting point is a *first quantized* representation of the

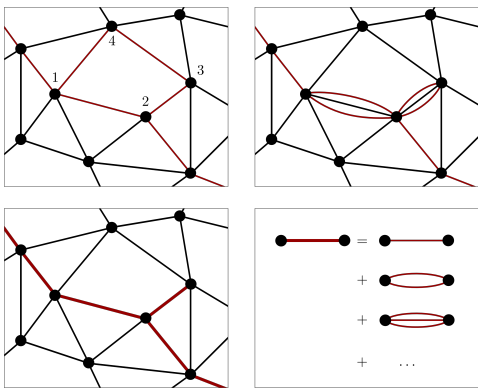


FIG. 5: Top left: a cartoon representation of a subset of sites in Fock space connected by a hopping amplitude containing a loop insertion. The four hopping amplitudes constituting the loop come with four independent energy denominators. Top right: this fourth order hopping amplitude with site revisits has only two independent energy denominators and contributes parametrically stronger. Bottom left: hopping amplitudes resummed according to the procedure shown in the bottom right.

problem, where we think of Fock space as a lattice with sites  $n$ , on-site energies,  $v_n$ , and a complicated random off-diagonal operator  $\hat{H}_4$  describing hopping between sites  $n, m$  with Hamming distance  $|n - m| = 2, 4$ . Statistically, hopping between sites differing in four fermion occupation numbers is much more likely to occur than hopping between sites with distance two, and we focus on the former throughout. In this way, the problem is described by high dimensional lattice model and key results on Anderson localization can be lifted from the existing work.

In the literature, localization in high dimensions has been considered on synthetic lattice types such as Bethe lattices [17, 23] or random regular graphs [16, 17, 21, 24] (meant to mimic the complexity of genuine Fock spaces). One usually introduces disorder via randomly chosen local site energies and considers uniform hopping between nearest neighbor sites. A competition between the high graph connectivity, and the impedance of transport due to randomly varying energy denominators then induces an Anderson transition at a critical combination of hopping strength, disorder, and graph coordination number [35].

Instead, we here work directly in Fock space and work with site connectivities defined by the native Hamiltonian (visualized in the cartoon of Fig. 2.) In this way, we arrive at a model with strongly fluctuating inter-site connectivity. What helps to keep this more complicated problem under control is the huge effective lattice coordination number of  $\mathcal{O}(N^4)$ , and a simplification known as the ‘effective medium approximation’ [35]. This approximation is commonly applied in the discussion of Anderson localization on high dimensional lattices and backed by their large coordination numbers. It describes

	site disorder	state extension	spectral statistics
I	$\delta < N^{-1/2}$	D	Wigner-Dyson
II	$N^{-1/2} < \delta \ll 1$	$\frac{D}{\sqrt{N\delta}}$	Wigner-Dyson
III	$1 < \delta \ll N^2$	$\frac{D}{\sqrt{N\delta^2}}$	Wigner-Dyson
IV	$N^2 < \delta$	$\mathcal{O}(D^0)$	Poisson

TABLE I: Summary of regimes with different wave function and spectral statistics.

transport as a process avoiding local loops (see Fig. 5), while multiple link traversals (top right) are included. The rationale behind this simplification is that at any given order in hopping perturbation theory, amplitudes with the lowest number of statistically independent energy denominators contribute the strongest. (Note that this assumption is hard wired into the phenomenological description via loop-less Bethe lattices from the outset.) The effective medium approximation sums over all transition amplitudes avoiding loops, but including multiple traversal of links (Fig. 5 bottom). Its application to the SYK lattice, detailed in section VI, sums these processes via recursion relations such as Eq. (40) whose solution leads to the final result Eq. (F3). One may optimistically hope that similar strategies can be generalized to the analysis of genuine MBL problems with spatial extension.

In summary, we arrive at the conclusion of four different regimes summarized in table I. In the rest of the paper, we discuss how these results are obtained from a matrix integral by methods developed in the theory of quantum disorder and localization.

### III. MATRIX MODEL

We start the derivation of the results summarized above by constructing an exact matrix integral representation of the correlation functions introduced above to describe many body wave functions and spectra. As mentioned in the previous section, the principal, and somewhat unconventional, perspective of this approach is a first quantized representation of the problem: we think of the SYK Hamiltonian as a big matrix, and treat it like that. Unlike in conventional approaches to many body problems, there will be no second quantized representation of Fock space. In this section, we discuss the construction of a matrix integral representing the theory averaged over SYK<sub>4</sub> disorder. The physics behind this formulation and that of a subsequent stationary phase analysis of the theory will be discussed in the next section.

All information on spectra and wave functions of the system is contained in the Fock space matrix elements of resolvent operators,

$$G_{nm}^{\pm} = \langle n | (z_{\pm} - \hat{H})^{-1} | m \rangle, \quad (16)$$

where  $z_{\pm} = \pm(\frac{\omega}{2} + i\eta)$  and, here and throughout,  $\eta$  is infinitesimal (with a limit  $\eta \searrow 0$  to be taken in the final step of all calculations). Specifically, the correlation functions above are obtained as

$$I_q = \frac{(2i\eta)^{q-1}}{2i\pi\nu} \sum_n \langle G_{nn}^{+(q-1)} G_{nn}^- \rangle,$$

$$K(\omega) = \frac{1}{2\pi^2\nu^2} \sum_{nm} \text{Re} \langle G_{nn}^+ G_{mm}^- \rangle, \quad (17)$$

where  $I_q$  is computed at  $\omega = 0$ , and  $\langle \dots \rangle$  denotes the average over matrix elements  $\{J_{ijkl}\}$ .

*Construction of the matrix integral.* — Following standard protocols, we raise the Green functions to an exponential representation before performing the Gaussian average. The basic auxiliary formula in this context is  $M_{nm}^{-1} = \int D(\bar{\psi}, \psi) e^{-\bar{\psi} M \psi} \psi_m^\sigma \bar{\psi}_n^\sigma$ , where  $M$  is a general  $L \times L$  matrix and the  $2L$  dimensional ‘graded’ vector  $\psi = (\psi^b, \psi^f)^T$  contains  $L$ -commuting components  $\psi_n^b$ , and an equal number of Grassmann components  $\psi_n^f$ . The double integral over these variables cancels unwanted determinants  $\det(M)$ , while the pre-exponential factors, either commuting or anti-commuting,  $\sigma = b, f$ , isolate the inverse matrix element. With the identification  $M = \text{diag}(-i[G^+]^{-1}, i[G^-]^{-1}) = -i\sigma_3(E + z - \hat{H})$ , we are led to consider the generating function

$$\mathcal{Z}[j] = \int D(\bar{\psi}, \psi) \left\langle e^{-\bar{\psi}(E+z-\hat{H}-j)\psi} \right\rangle_{\hat{H}_4}. \quad (18)$$

Here,  $z \equiv (\frac{\omega}{2} + i\eta) \sigma_3$ , contains the energy arguments of the Green functions and  $\sigma_3$  is a Pauli matrix distinguishing between advanced and retarded components. The matrix  $j$  acts as a source for the generation of the required moments of Green function matrix elements. Specifically, we define

$$j_K(\alpha, \beta) = \alpha \pi^b \otimes \pi^+ + \beta \pi^f \otimes \pi^-, \quad (19)$$

$$j_{I,n}(\alpha, \beta) = j_K(\alpha, \beta) \otimes |n\rangle\langle n|, \quad (20)$$

where  $\pi^{b,f}$  is a projector onto commuting and anticommuting-variables, respectively,  $\bar{\psi} \pi^\sigma \psi = \bar{\psi}^\sigma \psi^\sigma$ , and  $\pi^\pm$  projects in causal space,  $\bar{\psi} \pi^s \psi = \bar{\psi}^s \psi^s$ ,  $s = \pm$ . With these definitions, an elementary computation shows that

$$K(\omega) = \frac{1}{2\pi^2\nu^2} \text{Re} \partial_{\beta\alpha}^2 \mathcal{Z}[j_K] |_{\alpha,\beta=0}, \quad (21)$$

$$I_q = c_q (2i\eta)^{q-1} \sum_n \partial_\beta \partial_\alpha^{q-1} \mathcal{Z}[j_{I,n}] |_{\alpha,\beta=0}, \quad (22)$$

with  $c_q \equiv 1/(2i\pi\nu(q-1)!)$ . In the following, we consider the sources absorbed in a redefined energy matrix,  $z \rightarrow z - j$ , and remember their presence only when needed.

At this point, the averaging over  $\hat{H}_4$  can be performed, and it generates a quartic term

$$\mathcal{Z} = \int D(\bar{\psi}, \psi) e^{-\bar{\psi} \hat{G}^{-1} \psi + \frac{\omega^2}{2} \sum_a (\bar{\psi} \hat{X}_a \psi)^2}, \quad (23)$$

where we defined  $w^2 = 6J^2/(2N)^3 \equiv \frac{3}{2}N^{-4}$  for the scaled variance of the SYK Hamiltonian,  $\hat{G} \equiv (E + z - \hat{H}_2)^{-1}$ ,

$$\hat{X}_a \equiv \hat{\chi}_i \hat{\chi}_j \hat{\chi}_k \hat{\chi}_l, \quad (24)$$

and  $a = (i, j, k, l)$  with  $i < j < k < l$ . We next perform an innocuous but physically meaningful (see next section) rearrangement  $(\bar{\psi} \hat{X}_a \psi)^2 = \text{STr}((\bar{\psi} \hat{X}_a \psi)^2)$ , where the supertrace [35]  $\text{STr}(X) \equiv \text{tr}(X^{\text{bb}}) - \text{tr}(X^{\text{ff}})$  accounts for the minus sign caught when exchanging anti-commuting variables. The next step is a Hubbard-Stratonovich transformation decoupling the matrices  $\bar{\psi} \hat{X}_a \psi \sim A_a$  in terms of  $(2N)^4/4!$  auxiliary matrix fields  $A_a$ . Referring for details of the procedure to Appendix A we note that after the decoupling the the integral over  $\psi$ -variables has become Gaussian and can be carried out. A more interesting statement is that of the  $\rho \equiv \binom{2N}{4}$  Hubbard-Stratonovich fields  $A_a$ , all but one can be removed, too, by straightforward Gaussian integration. Upon restricting to  $E = 0$  this leaves us with a single integration,

$$\mathcal{Z} = \int \mathcal{D}Y e^{-S[Y]}, \quad (25)$$

$$S[Y] = -\frac{1}{2} \text{STr}(Y \mathcal{P} Y) + \text{STr} \log \left( z - \hat{H}_2 + i \mathcal{P} Y \right),$$

over a  $2 \times 2 \times \times D$  dimensional matrix  $Y = \{Y_{nn'}^{\sigma\sigma'}\}$  carrying indices in causal space, super-space, and Fock space. The information on the SYK system now sits in the site-diagonal one-body term,  $\hat{H}_2$ , and the hopping operator  $\mathcal{P}$  which represents the interaction and acts on matrices  $Z = \{Z_{nm}\}$  in Fock space as

$$\mathcal{P} Z \equiv \frac{1}{\rho} \sum_a X_a Z X_a^\dagger. \quad (26)$$

Finally,  $\gamma = w\rho^{1/2} = 1$  represents the SYK<sub>4</sub> band width, which we have set to unity. To simplify formulas, we will consider energies  $\hat{H}_2 \rightarrow \gamma \hat{H}_2$ ,  $\omega \rightarrow \gamma\omega$  scaled by this parameter, and suppress it throughout.

*Discussion of the matrix integral.* — This is now a good point to discuss the meaning of the above Hubbard-Stratonovich transformation and of the matrix-representation. The two-fermion vertices  $\bar{\psi} \hat{X}_a \psi$  entering the theory after disorder averaging describe the scattering of Fock space states off the four-Majorana operators contained in the Hamiltonian, and in this way introduce the lattice connectivity indicated in Fig. 1. While a direct analysis of individual Fock space amplitudes seems hopeless, progress can be made if the propagators are paired to two-amplitudes composites as indicated in Fig. 6. For two reasons, the pair amplitudes  $Y_{nn'}^{ss',\sigma\sigma'} = \bar{\psi}_n^{s\sigma} \bar{\psi}_{n'}^{s'\sigma'}$  are more convenient degrees of freedom: First, the pair action  $Y \rightarrow \sum_a \hat{X}_a Y \hat{X}_a = \rho \mathcal{P} Y$  governing scattering in the two-state channel (cf. the structure of the action (25)) is relatively easy to describe, see below. Second, the advanced/retarded combinations  $Y_{nn}^{-+,\sigma\sigma'} = \bar{\psi}_n^{-\sigma} \bar{\psi}_n^{+\sigma'}$  appear as terminal vertices in the computation of Green

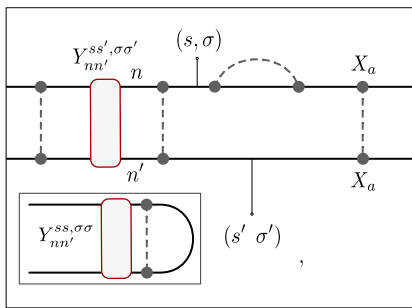


FIG. 6: The composite matrix degree of freedom  $Y_{nn'}^{ss',\sigma\sigma'}$  representing the pair propagation of Fock space scattering amplitudes. Discussion, see text.

functions  $G_n^+ G_n^-$ , where the dots stand for the unspecified final points of the correlation function. With the exact identity  $(G^+)^{-1} - (G^-)^{-1} = \omega^+ \equiv \omega + 2i0$ , we have  $\langle G_{mn}^+ G_{nm}^- \rangle = \langle \text{tr}(G^+ G^-) \rangle = \frac{1}{\omega^+} \langle \text{tr}(G^+) [(G^+)^{-1} - (G^-)^{-1}] G^- \rangle = \frac{1}{\omega^+} \langle \text{tr}(G^- - G^+) \rangle \simeq \frac{2\pi i}{\omega^+} \nu$ , where  $\nu$  is the density of states at the band center. The way to read this (Ward) identity is that the product of Green functions contains a singularity, *provided*  $\text{tr}(G^- - G^+) \sim \nu$  is a structureless quantity. (The latter condition does not hold in systems with localization, where the isolated eigenstates support a point spectrum with poles rather than a uniform cut.) This argument indicates that the ‘soft mode’  $G^+ G^- \sim \omega^{-1}$  is key to the understanding of observables probing spectrum and eigenfunctions of the system.

In the matrix integral framework, the above singularity shows in the presence of a soft mode in the integration over the variables  $Y_{nn'}^{-+,\sigma\sigma'}$ . To isolate this mode, we note that Eq. (25) has an approximate symmetry

$$Y \rightarrow TYT^{-1}, \quad T = \{T^{ss',\sigma\sigma'}\} \quad (27)$$

under rotations homogeneous in Fock space. The set of these transformations defines  $\text{GL}(2|2)$ , i.e. the group of invertible  $4 \times 4$  matrices with anti-commuting entries. Invariance under this symmetry is weakly broken only by the frequency/source matrix  $z$ , which, ignoring the infinitesimal sources, transforms as  $\frac{\omega}{2}\sigma_3 \rightarrow \frac{\omega}{2}T^{-1}\sigma_3T$ . This reduces the symmetry down to the transformations diagonal in advanced-retarded ( $s$ -indices) space,  $\text{GL}(1|1) \times \text{GL}(1|1)$ .

The essential question now is whether the above weak explicit symmetry breaking is *spontaneously broken* in the matrix integral (much as a weak explicit symmetry breaking by a finite magnetic field gets upgraded to spontaneous symmetry breaking in a ferromagnetic phase.) In the latter case, we expect a soft Goldstone mode whose ‘mass’ is set by the symmetry breaking parameter,  $\omega$ , and  $\omega^{-1}$  singularities in line with the observation above. To investigate this question and the consequences in the observables  $K(\omega)$  and  $I_q$ , we next subject the theory to a stationary phase analysis.

#### IV. EFFECTIVE THEORY

In this section, we map the exact theory Eq. (25) to an approximate but more manageable effective theory. We have already established the presence of an exact (in the limit  $\omega \rightarrow 0$ ) rotational soft mode isotropic in Fock space. Since much of the analysis below will focus on strong  $\hat{H}_2$  with eigenvalues  $v_n$  of  $\hat{H}_2$  comparable to or exceeding the SYK<sub>4</sub>, we anticipate that fluctuations of lowest action cost will be commutative in the sense  $[\hat{H}_2, Y] = 0$ . We thus start from an ansatz  $\langle n|Y|m\rangle = Y_n \delta_{nm}$  where fluctuations are diagonal in the occupation basis. In view of the fermion parity conservation of both  $\hat{H}_{2,4}$  we focus on a sector of definite parity, chosen to be even. The locality of  $\hat{H}_2$  in the occupation number basis is in competition with the hopping described by  $\mathcal{P}$ . However, what works to our advantage is that the action of  $\mathcal{P}$  on the states  $Y$  is remarkably simple: thinking of  $Y_{nm}$  as the matrix elements of a ‘density matrix’,  $Y_n$  represents a state without off-diagonal matrix elements. It is a non-trivial feature of  $\mathcal{P}$  that it preserves this structure,  $(\mathcal{P}Y)_m = \sum_n \mathcal{P}_{|n-m|} Y_m$ , i.e. the adjoint action  $\hat{X}_a Y \hat{X}_a$  on Fock-space diagonal matrices  $Y$  does not generate superpositions of off-diagonal states. A straightforward combinatorial exercise shows that (see Appendix B for details)

$$\mathcal{P}_0 = \frac{N(N-1)}{2\rho}, \quad \mathcal{P}_2 = \frac{4(N-2)}{\rho}, \quad \mathcal{P}_4 = \frac{16}{\rho}, \quad (28)$$

with all other matrix elements vanishing, and normalization  $\sum_m \mathcal{P}_{m,n} = 1$ . Notice that for a given  $n$ , we have  $\binom{N}{4}$  neighbors with hamming distance 4, connected to  $n$  by  $\binom{N}{4} \mathcal{P}_4 \stackrel{N \gg 1}{\approx} 1$ . This shows distance 4 hopping is the most important by ‘phase volume’.

With these structures in place, a variation of action (25) leads to

$$-iY = \frac{1}{z - \hat{H}_2 + i\mathcal{P}Y}. \quad (29)$$

Notice that  $Y$  resembles  $(-i)$  times the local ‘propagator’ (see inset of Fig. 6) of site  $n$ , dressed with a self energy  $i\mathcal{P}Y$  due to hopping via  $\mathcal{P}$  to neighboring sites. It is this term which makes the stationary phase equation non-trivial. In a first step towards the solution, we neglect imaginary contributions to  $Y$  and focus on the local ‘spectral density’  $\text{Re}(Y)$  instead. (In the effective action, the imaginary part of  $Y$  describes an energy shift  $v_n \rightarrow v_n + \text{Im}Y_n$  which is inessential to our problem.) Causality requires  $\text{sgn} Y = \text{sgn} \text{Im} z$ , i.e. the sign of the self energy is dictated by that of the imaginary part contained in the energy arguments. Otherwise the saddle point equation is rotationally invariant in the internal indices of the theory. This motivates an ansatz,

$$\text{Re} Y = \sum_n (\text{Re} Y)_n |n\rangle \langle n| \equiv \sum_n \pi \nu_n |n\rangle \langle n| \otimes \sigma_3 \otimes \mathbb{1}_{\text{bf}}$$

with real coefficients  $\nu_n$ . Inspection of Eq. (29) shows that these coefficients afford an interpretation as mean field local density of states.

Substituting this expression into the equation and temporarily ignoring the small energy argument,  $z$ , as small compared to both  $\hat{H}_2$  and  $Y$ , we obtain the variational equation (5). The structure of this equation contains the key to its solution: For  $v_n = 0$ , the normalization  $\sum_m \mathcal{P}_{|n-m|} = 1$  implies that it is solved by  $\kappa_n = 1$ . In the chosen units, this is  $(\pi \times)$  the density of states at the SYK band center. For finite  $v_n$ , the summation over  $m$  implements an effective average over the connected states, which now carry random energy. In Appendix C we show that the average stabilizes the solution (6), where ‘ $\simeq$ ’ stands for equality up to corrections exponentially small in  $\exp(-(v_n/\delta)^2)$ . We interpret this result as the spectral density of sites with energy  $v_n$  and decay rate  $\kappa_n$  into neighboring sites. The latter is finite for states below a threshold  $|v_n| < C$ . For  $\delta > 1$ , the rate is given by the energy denominator  $\kappa \sim \delta^{-1}$  of neighboring sites. In the opposite regime,  $\delta < 1$ , the energy denominators of states  $v_n \sim 1$  in resonance with the SYK band width are of  $\mathcal{O}(1)$ , leading to the second line in Eq. (6).

The saddle point solutions discussed thus far are distinguished for their diagonality in all matrix indices. However, we now recall that the  $z = 0$  action is invariant under Fock space uniform rotations Eq. (27), implying that uniformly rotated saddle point configurations  $Y_n \rightarrow T Y_n T^{-1}$  are solutions, too. (Technically, this follows from the cyclic invariance of the trace.) Next to this uniform Goldstone mode, configurations  $Y_n \rightarrow T_n Y_n T_n^{-1}$  with site-diagonal rotations commutative with  $\hat{H}_2$  are expected to cost the least amount of action. With  $Y_n = \pi \nu_n \sigma_3$ , this makes  $Y_n \rightarrow \pi \nu_n Q_n$ ,  $Q_n = T_n \sigma_3 T_n^{-1}$  the effective degrees of freedom of the theory, and substitution into Eq. (25) defines the Goldstone mode integral,

$$\mathcal{Z} = \int \mathcal{D}Q e^{-S[Q]}, \quad (30)$$

$$S = -\frac{\pi^2}{2} \text{STr}((\hat{\nu}\hat{Q})\mathcal{P}(\hat{\nu}\hat{Q})) + \text{STr} \log \left( z - \hat{H}_2 + i\pi\mathcal{P}(\hat{\nu}\hat{Q}) \right).$$

In the next two sections, we investigate what this integral has to say about wave function statistics and Fock space localization, respectively.

## V. SPECTRAL AND WAVE FUNCTION STATISTICS

In this section, we explore the spectral and wave function statistics in regimes I-III. The presumption is that wave functions are not yet localized and correlated with each other. This should lead to Wigner-Dyson spectral statistics and wave function moments reflecting the extended nature on the subsets of Fock space corresponding to active or resonant sites.

To test these hypothesis it is sufficient to consider the integral (30) in the presence of effectively infinitesimal ex-

PLICIT symmetry breaking  $z$ : besides the sources,  $j$ , this parameter contains a frequency argument  $\omega \sim D^{-1}$  of the order of the exponentially small inverse many body level spacing in the case of spectral statistics, Eq. (21), or the infinitesimal parameter  $\eta$  in the case of wave function statistics, Eq. (22). On general grounds, we expect the smallness in the ‘explicit’ symmetry breaking in a Goldstone mode integral to lead to singular contributions  $\sim z^{-n}$  proportional in the inverse of the that parameter after integration. (Inspection of the prefactors,  $\eta^{q-1}$  in the definition of the wave function statistics shows that such singularities are actually required to obtain non-vanishing results.) These most singular contributions to the integral must come from the Goldstone mode fluctuations of least action, which are fluctuations homogeneous in Fock space,

$$\hat{Q}_n = T_n \sigma_3 T_n \rightarrow T \sigma_3 T^{-1} \equiv Q. \quad (31)$$

With  $[T, \mathcal{P}] = 0$ , the substitution  $\hat{\nu}\hat{Q} \rightarrow \hat{\nu}Q$  into the action Eq.(30) leads to

$$S_0[Q, j] = \text{STr} \log \left( z - j - \hat{H}_2 + i\hat{\kappa}Q \right), \quad (32)$$

where we made the dependence  $z \rightarrow z - j$  of the action on the sources  $j \equiv j_{I,n}$  required to calculate moments via Eq. (20) explicit again, and we noted  $\pi\mathcal{P}\hat{\nu} = \hat{\kappa}$ .

Before proceeding, we note that the structure of this action is identical to that describing the Rosenzweig-Porter model — a single random matrix of dimension  $D$  containing Gaussian distributed disorder on the matrix diagonal [48]. An important difference is, however, that the diagonal disorder in the latter is uncorrelated, while the Fock-space diagonal disorder induced by  $\hat{H}_2$  is highly correlated. As a consequence, the effective action for the Rosenzweig-Porter model only allows for homogenous saddle point solutions [36, 48], while here we encounter solutions that become inhomogeneous in Fock space once on-site disorder exceeds the SYK<sub>4</sub> band width. The inhomogeneity accounts for a site-dependent broadening  $\kappa_n$ , induced by correlations in the disorder amplitudes, and also manifests in a separation into regimes II/III of the regime of non ergodic extended states. In the following, we discuss what this reduction of the model has to say about spectral and wave function statistics.

### A. Spectral statistics

To obtain a prediction for spectral correlations based on the representation Eq. (30) with Fock space zero mode, we consider the correlation function (7), represented through matrix integral represented Green functions as in Eq. (17) and Eq. (21). To compute these quantities from the effective theory, we need to expand the action Eq. (32) to lowest order in the parameter  $\omega/\kappa \sim 1/D$ , and to second order in the sources (19).

The straightforward  $\omega$ -expansion yields (cf. Eq. (D3))

$$S_\omega[Q] \equiv -i \frac{\pi\nu(\omega + i\eta)}{2} \text{STr}(Q\sigma_3), \quad (33)$$

where  $\nu$  is the zero energy density of states, Eq. (10). What remains, is the source differentiation and the integration over the matrix  $Q$ . To get some intuition for the integral, notice that the non-linear degree of freedom  $Q = T\sigma_3 T^{-1}$  affords a representation,  $Q = UQ_0U^{-1}$ , where  $U$  contains various compact angular variables (cf. Appendix E), and

$$Q_0 = \begin{pmatrix} \cos \hat{\theta} & i \sin \hat{\theta} \\ -i \sin \hat{\theta} & -\cos \hat{\theta} \end{pmatrix}, \quad (34)$$

a rotation matrix in causal space. Diagonal in super-space, this matrix is parameterized in terms of the two ‘Bogolubov’ angles  $\hat{\theta} = (i\theta_b, \theta_f)^T$ , where  $\theta_f \in [0, \pi]$  is a compact rotation variable, and  $\theta_b \in \mathbb{R}^+$  a non-compact real variable. This representation reveals the geometry of the integration manifold as the product of a sphere ( $\theta_f$ ) and a hyperboloid ( $\theta_b$ ) (coupled by variables contained in  $U$ .) Where the physics of non-perturbative structures in spectral and wave function statistics, and localization is concerned, the most important player is the non-compact variable,  $\theta_b$ , as only this one has the capacity to produce singular results. Heuristically, one may think of the model reduced to its dependence on this variable as a non-compact version of a Heisenberg-model, containing hyperboloidal, rather than compact spins as degrees of freedom.

Referring for details of the source differentiation and the subsequent integration over the matrix  $Q$  [35] to Appendix E, the above reduction of the model yields the GUE spectral correlation function (9) for the spectral statistics on scales of the many body level spacing in regimes I-III. With increasing energies, the assumption of homogeneity of fluctuations in Fock space breaks down (cf. the next section) beyond a ‘Thouless energy’ whose value depends on the specific observable under consideration [49]. However, the detailed investigation of Thouless thresholds for the present model is beyond the scope of the paper.

## B. Wave function statistics

In the same manner, we may consider the local moments of wave functions Eq. (8), represented via Green functions Eq. (17), and obtained from the matrix integral through Eq. (22). A key feature of this expression is that it contains a limit  $\lim_{\eta \rightarrow 0} \eta^{q-1}(\dots)$  the factor  $\eta^{q-1}$  must thus be compensated for by an equally strong singularity  $\eta^{1-q}$  from the integral, where  $\eta$  couples through  $z = i\eta\sigma_3$ . Setting  $\omega = 0$  in Eq. (33) and integrating over the functional differentiated in sources a calculation detailed in Appendix E), then yields the moments (12)–(14).

The support of wave functions in regimes II and III is different (as indicated by the different value of  $D_{\text{res}}$  in Eqs. (14)), while the DoS Eq. (10) assumes the same value. The reason for this is that, in regime II, there is no distinction between active and resonant sites: there are  $\sim D/(\sqrt{N}\delta)$  active sites contributing with unit weight to the DoS. By contrast, in III, the dominant contribution to the DoS comes from the smaller number of  $D_{\text{res}} \sim D/(\sqrt{N}\delta^2)$  resonant sites, with sharply peaked spectral weight  $\sim \delta$ ,  $\nu \sim D_{\text{res}}\delta \sim D/(\sqrt{N}\delta)$ . In this

## C. Comparison to numerics

To numerically check the predictions for the statistics of many body wave functions and spectra, we calculated eigenfunctions and spectrum from exact diagonalization of the Hamiltonian  $\hat{H} = \hat{H}_4 + \hat{H}_2$ , see (1) and (3), for  $\{v_i\}$  obtained by diagonalizing (2) as a one-body problem, for  $2N = 22, 26, 30$  Majorana fermions and varying values of  $\delta$ . We kept 1/7 of the total spectrum and verified both a nearly constant density of states and that results remain unchanged when we restrict to a smaller energy window. From the selected eigenfunctions in the center of the band, we calculated statistics of the moments of the wave function according to Eq. (8). The eigenfunctions are normalized in each definite parity subspace. For the spectrum we compared the numerical statistical distribution with both Wigner-Dyson and Poisson distributions by calculating the Kullback-Leibler divergence,  $KL \equiv D(P||Q) = \sum_k p_k \log(\frac{p_k}{q_k})$ , where  $p_k$  is the spectral statistics from numerical data and  $q_k$  the respective distribution. In order to avoid level unfolding, we followed Ref. 46 and studied the statistics of ratios of energy spacings,  $r_j = \min(\frac{s_j}{s_{j-1}}, \frac{s_{j-1}}{s_j})$ , where  $s_j = e_{j+1} - e_j$  is the nearest neighbor spacing of the eigenenergies  $\{e_j\}$ . The  $q_k$  are then given by numerically integrating either the Wigner-Dyson or the Poisson distribution for the variable  $r$  over each bin centered at  $r_k$ , given by Ref. 50,

$$P(r) = \begin{cases} \frac{81\sqrt{3}}{2\pi} \frac{(r+r^2)^2}{(1+r+r^2)^4} + \delta P(r), & \text{Wigner-Dyson (GUE),} \\ \frac{2}{(1+r)^2}, & \text{Poisson,} \end{cases} \quad (35)$$

where  $\delta P$  is a numerical correction given by  $\delta P = \frac{2C}{(1+r)^2} [(r+1/r)^{-2} - c_2(r+1/r)^{-3}]$ , with  $c_2 = 4(4-\pi)/(3\pi-8)$  and  $C = 0.578846$  is obtained from fitting numerical results in the GUE [50].

In all figures the numerical values result from averaging over eigenvectors and spectrum, taken from the band center and from both parity sectors, of at least 1000 independent realizations of the model. In computing the Kullback-Leibler divergence, the numerical distribution for  $r_j$  is obtained by splitting the interval  $[0, 1]$  into 50 bins of equal widths.

## VI. EXTENDED-TO-LOCALIZED TRANSITION

In regimes, II, III, the dominant contribution to the matrix integral at the lowest energies comes from homogeneous contributions  $Q$ . Upon approaching the localization threshold III/IV, inhomogeneous fluctuations  $Q \rightarrow \hat{Q} = \{Q_n\}$  gain in importance and eventually destabilize the mean field theory. To describe this physics, we need an effective action generalized for inhomogeneous fluctuations, and more manageable than Eq. (30). We derive it in Appendix D under the assumption that the sum over a large number of fluctuating terms represented by the term  $\mathcal{P}(\hat{\nu}\hat{Q})$  is largely self-averaging. An expansion to lowest order in fluctuations around the homogeneous average than leads to the effective hopping action

$$S[Q] = S_{\mathcal{P}}[Q] + S_{\omega}[Q],$$

$$S_{\mathcal{P}}[Q] = \frac{\pi^2}{2} \sum_{n,m} \nu_n \nu_m \mathcal{P}_{n,m} \text{Str}(Q_n Q_m), \quad (36)$$

$$S_{\omega}[Q] = -i\pi \sum_n \nu_n \text{Str}(zQ_n), \quad (37)$$

with  $Q_n = T_n^{-1} \sigma_3 T_n$  and ‘Str’ traces only over internal degrees of freedom. Eqs. (36) and (37) are the main result of this section. Depending on the value of  $\kappa_n$  Eq. (6), this action describes the entire range from vanishing to large deformations  $\hat{H}_2$ . We next discuss what this action has to say on the ergodic-to-localization transition.

The key player in this problem is the hopping term (36) where  $Q$  matrices at SYK<sub>4</sub>-neighboring sites are coupled, subject to a weight which contains the local spectral densities. In analytic approaches to localization on high dimensional lattices, it is common to set these weights to unity. However, in view of the massive site-to-site fluctuations of  $\nu_n$  we prefer not to make this assumption and work with a given realization  $\{\nu_n\}$  for as long as possible. Approaching the transition from the localized side where the integration over  $Q$ ’s is subject to only small damping  $\nu_n$ , the essential degrees of freedom are once again the non-compact variables,  $\theta_b$ , contained in  $Q_0$ , Eq. (34).

To better understand the significance of this structure, we write  $Q_n Q_m = (Q_n - \sigma_3)(Q_m - \sigma_3) + \sigma_3 Q_n + \sigma_3 Q_m - \mathbb{1}$  to represent the hopping part of the action as

$$S_{\mathcal{P}}[Q] = \pi \sum_n \Gamma_n \text{Str}(Q_n \sigma_3) + \frac{\pi^2}{2} \sum_{n,m} \nu_n \nu_m \mathcal{P}_{n,m} \text{Str}((Q_n - \sigma_3)(Q_m - \sigma_3)),$$

where  $\Gamma_n \equiv \nu_n \sum_m \mathcal{P}_{n,m} \nu_m$ . Consider a situation where the accumulate hopping weights  $\Gamma_n$  out of site  $n$  are small. In this case, large fluctuations of the non-compact angles,  $\lambda_{b,n} \equiv \cosh(\theta_{b,n})$  dominate the functional integral. To understand the consequences, we note that the measure of the  $Q$ -integration in the angular representa-

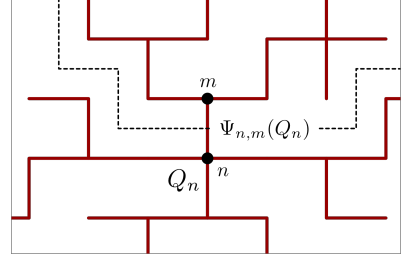


FIG. 7: Idea of the effective medium approximation. Sites  $n$  are connected to the stems of coral like structures, each labeled by a connected neighbor  $m$ , which represent the summation over all hopping terms excluding loops. The recursive nature of the structure allows for a self consistent resummation.

tion is given by [35]

$$\int dQ = \int dU \int_{-1}^1 d\lambda_f \int_1^{\infty} d\lambda_b \frac{1}{(\lambda_b - \lambda_f)^2},$$

where  $\lambda_f = \cos(\theta_f)$ . For small typical values  $\Gamma \sim \Gamma_n \ll 1$ , the exponential weighs effectively cut off the integration over  $\lambda_b$  at  $\sim \Gamma^{-1} \gg 1$ . Individual terms in the second line of the above representation of  $S_{\mathcal{P}}$  are smaller than the accumulated weights in the first line, and so the integral can be approached by perturbative expansion in the hopping terms. As an example, consider the sixth order expansion indicated via the highlighted links in Fig. 5. Retaining only the information on the non-compact integrations  $\lambda \equiv \lambda_b$ , the contribution with a loop (left) and that with doubly occurring links evaluate to

$$\text{loop: } \int_1^{\Gamma^{-1}} \frac{d\lambda_1}{\lambda_1^2} \frac{d\lambda_2}{\lambda_2^2} \frac{d\lambda_3}{\lambda_3^2} \frac{d\lambda_4}{\lambda_4^2} \lambda_1^3 \lambda_2^3 \lambda_3^2 \lambda_4^2 \sim \Gamma^{-6},$$

$$\text{no loop: } \int_1^{\Gamma^{-1}} \frac{d\lambda_1}{\lambda_1^2} \frac{d\lambda_2}{\lambda_2^2} \frac{d\lambda_3}{\lambda_3^2} \lambda_1^3 \lambda_2^5 \lambda_3^2 \sim \Gamma^{-7}, \quad (38)$$

where the indices refer to the participating  $Q$ -matrices,  $Q_{1\dots 4}$ . This estimate shows that the contribution of loops in the perturbation expansion is suppressed. At the same time, the largeness of the individual contributions signals that infinite order summations are required. The effective medium approximation achieves this summation, loops excluded. The approximation is called ‘effective medium’ because from the perspective of individual sites in Fock space the contribution of all hopping processes terminating at that site adds up to the influence of an effectively homogeneous background medium, transmissive or not depending on the strength of the couplings.

To see how this comes about, consider a site  $n$  with local configuration  $Q_n$  and let  $\Psi_{n,m}(Q_n) = \int_{\text{coral } m, Q} DQ e^{-S[Q]}$ , be the contribution to the functional integrated over all links connected to  $n$  via the neighbor  $m$ , through the loopless coral like structure indicated in Fig. 7. The essence of the approximation is

the recursion relation,

$$\Psi_{nm}(Q) = \int dQ' N_{w_{nm}}(Q, Q') e^{-S_0(Q')} \prod_o \Psi_{mo}(Q'),$$

$$N_w(Q, Q') = e^{w \text{Str}(QQ')},$$

where the product extends over all sites,  $o$ , connected to  $m$  by hopping,  $S_0(Q) \equiv S_{\omega \rightarrow i\delta}(Q)$  acts as a convergence generating factor, and we defined

$$w_{nm} \equiv \frac{\pi^2}{2} \nu_n \nu_m \mathcal{P}_{n,m}, \quad (39)$$

for the coupling constants weighting the hopping kernel. If we now take the product  $\Psi_n(Q) \equiv \prod_m \Psi_{n,m}(Q)$  (assuming self averaging in the sense that the fully integrated amplitude,  $\Psi_n$  depends on the terminal site,  $n$ , but not on the detailed values of the  $\mathcal{O}(N^4)$  neighbor amplitudes), the equation assumes the form,

$$\Psi_n(Q) = \prod_m \int dQ' N_{w_{n,m}}(Q, Q') \Psi_m(Q'),$$

where the presence of the convergence generator  $\exp(-S_0)$  is left implicit. In the deeply localized regime,  $N_{n,m} \approx 1$ , the integral decouples, and  $\Psi_n = 1$  is a solution by supersymmetry (i.e. the unit normalization of all source-less integrals in the present formalism). This suggests [35] a linearization,  $\Psi_n(Q) = 1 - \Phi_n(Q)$ , where the emergence of a non-trivial solution  $\Phi_n$  is taken as a criterion for the localization transition. Substituting this ansatz into the equation, and again using supersymmetry,  $\prod_m \int dQ' N_w(Q, Q') = 1$ , we obtain

$$\Phi_n(Q) = \sum_m \int dQ' N_{w_{nm}}(Q, Q') \Phi_m(Q'). \quad (40)$$

This is a linear integral equation governed by a random lattice structure in Fock space via the couplings  $w_{nm}$  and an internal structure encoding the randomness of the SYK<sub>4</sub> system via the  $Q'$ -integrals. Although the integral equation may look helplessly complicated, progress is possible recalling our previous observation: we again have a situation where the  $Q$  integrations extend over wide parameter intervals such that the leading non-compact variable is the key player. Assuming that the solutions depend on the non-compact variable as  $\Phi(Q) \rightarrow \Phi(t)$ ,  $t \equiv \log(\lambda_1/\delta)$ , and referring to Ref. [51] for details of the integration over remaining variables, the reduction of Eq. (40) to the regime of interest,  $t \ll 0$ ,  $w_{mn} \ll 1$  reads

$$\Phi_n(t) = \sum_m \int dt' L_{w_{mn}}(t-t') \Phi_m(t'), \quad (41)$$

$$L_w(t) = \left(\frac{w}{2\pi}\right)^{1/2} e^{-w \cosh(t) + \frac{t}{2}} \left(w \cosh t + \frac{1}{2}\right).$$

Ref. [51] contains a pedagogical discussion of the solution of (the homogeneous variant  $w_{mn} = \text{const.}$  of this equation, including the somewhat subtle issue of boundary

conditions. It turns out that the key to the stability of the localized solution,  $\Psi = 1$  lies in the spectrum of the linear kernel  $\{L_{w_{mn}}(t-t')\}$ : a spectrum with lower bound  $\epsilon > 1$  means that perturbations  $\delta\psi$  will grow under the application of the linearized kernel, signifying destabilization of the null solution  $\psi = 1$ . We thus declare the existence of a minimal eigenvalue  $\epsilon = 1$  as a delocalization criterion. Due to translational invariance in  $t-t'$  eigenstates are of the form  $e^{\theta(t-t')} \Phi_n$ , where the coefficients are determined by the reduced equation,  $\Phi_n = \sum_m L_{\theta,nm} \Phi_m$ , with

$$L_{\theta,nm} = \int_{-\infty}^{\infty} dt L_{w_{mn}}(t) e^{-\theta t}.$$

Substitution of the kernel in Eq. (41) followed by differentiation in  $\theta$  shows that the positive matrix  $L_{\theta,nm}$  assumes its smallest values at  $\theta = 1/2$ , and the straightforward integration at that value defines the matrix,

$$L_{nm} \equiv L_{\frac{1}{2},nm}$$

$$= \left(\frac{w_{nm}}{2\pi}\right)^{1/2} \int dt e^{-w_{nm} \cosh t} \left(w_{nm} \cosh t + \frac{1}{2}\right)$$

$$\simeq \left(\frac{w_{nm}}{2\pi}\right)^{1/2} \log\left(\frac{2}{w_{mn}}\right).$$

We thus arrive at the eigen equation

$$\Phi_n = \frac{2\sqrt{\pi}}{\sqrt{\rho}} \sum_{|n-m|=4} a_{nm} \Phi_m,$$

$$a_{nm} = \sqrt{\nu_n \nu_m} \log\left(\frac{\rho}{(2\pi)^2 \nu_n \nu_m}\right), \quad (42)$$

where the sum extends over  $Z \equiv \binom{N}{4}$  sites in Hamming distance four to the reference site  $n$  [52], and we recall that  $\rho \equiv \binom{2N}{4}$ . We read Eq. (42) as an equation for the existence of a unit eigenvalue whose solvability depends on the value of  $\delta$  determining the local density of states,  $\nu_n$ . In Appendix F we show that the summation in this equation is dominated by resonant sites, and how this simplifies its logarithmic dependence. Once again using the self averaging feature to replace the sum by an average over the distribution of  $\nu_m$ , we find that Eq. (42) has a solution for  $\delta = \delta_c$  determined by the criterion Eq. (F3). In the limit  $N \gg 1$  the latter simplifies to

$$\delta_c \simeq \frac{N^2}{4\sqrt{3}} \log N, \quad (43)$$

with the characteristic  $\delta_c \sim N^2 \ln N$  scaling first predicted in Ref. [2]. However, as discussed in section II, the numerical data for small values  $N = 10^1$  responds sensitively to such approximations and improved agreement is obtained by working with the solution Eq. (F3).

## VII. DISCUSSION

In this paper, we have presented a first principles analysis of Fock space localization in the Majorana SYK<sub>4+2</sub>

model, describing a competition of two-body interaction and one-body potential. Within this setting we provided a complete description from an ergodic regime, over an intermediary regime of non-ergodic extended states to the localized phase, all formulated in the eigenbasis of the one-body Hamiltonian. To the best of our knowledge, this is the only genuine many body system for which microscopic and analytical studies of many body localization are possible at this stage.

Many of the theoretical tools applied above to describe the localization phenomenon were originally developed for synthetic systems — such as Bethe lattices subject to disorder, or modified variants of random matrix theory — meant to mimic true Fock spaces. From a methodological perspective, the main contribution of the present paper is an adaption of these concepts to become applicable to a microscopically defined environment. The main ally in this extension was the large coordination number  $\sim N^4$  of the SYK Fock space which implied self averaging over microscopic details in quantitative agreement to parameter free numerical cross checks.

Referring to table I for a summary, we tested the predictions of the theory for the statistics of spectra and wave functions in the ergodic regime (I), and the strongly non-ergodic regime (III) by comparison to numerical data for systems of size  $N = 11 - 15$ . (For these systems, the parametric extension of an intermediate regime II of weak non-ergodicity was too narrow to be testable.) We saw clear indications of the Fock space Anderson transition in the finite size scaling of both wave function and spectral statistics, at a critical point which agrees with the theoretically predicted value up to a size-independent numerical constant of  $\mathcal{O}(1)$ . However, a quantitative analysis of critical exponents and finite size scaling is beyond the scope of this work.

Conceptually, the main contribution of this analysis is an effective theory for a many body localization problem whose predictions are backed by a variety of numerical checks for system sizes reachable on contemporary hardware. However, the scope of the analytical predictions is not limited in  $N$ , and this makes the model a promising building block to describe thermodynamic limits and, perhaps, higher-dimensional settings where the interplay of Fock space and real space extension defines the physics of the genuine MBL transition.

### Acknowledgments

Discussions with A. D. Mirlin, K. Tikhonov, and D. A. Huse are gratefully acknowledged. F. M and T. M. acknowledge financial support by Brazilian agencies CNPq and FAPERJ. The work of M. T. was partially supported by JSPS KAKENHI Grants JP17K17822, 20H05270 and JP20K03787. Work funded by the Deutsche Forschungsgemeinschaft (DFG, German Research Foundation) - Projektnummer 277101999 - TRR 183 (project A03). Part of the numerical computation in

this work was carried out at the Supercomputer Center, ISSP, University of Tokyo.

### Appendix A: Derivation of the action (25)

We here derive the action Eq. (25) from the averaged functional (23). We start by rewriting the quartic term as  $(\bar{\psi}\hat{X}_a\psi)^2 = \text{STr}((\psi\bar{\psi}\hat{X}_a)^2)$ . To decouple this nonlinearity, we multiply the functional with the unit normalized Gaussian integral  $1 = \int DA \exp(-\frac{1}{2}\sum_a \text{STr}(A_a\hat{X}_a)^2)$ , where  $DA \equiv \prod_a dA_a$ , and  $A_a = \{A_{nn'}^{ss'}\}$  are  $4D$ -dimensional matrices. A shift  $A_a \rightarrow A_a + w\psi\bar{\psi}$  then removes the quartic term, and the subsequent integration over  $\psi$  leads to

$$\mathcal{Z}[j] = \int DA e^{-\frac{1}{2}\sum_a \text{STr}(A_a\hat{X}_a)^2 - \text{STr} \log(\hat{G}^{-1} + w\sum_a A_a)},$$

where  $\hat{G}^{-1} = z - \hat{H}_2$ . We now observe that the nonlinear part of the action couples only to the combination  $\sum_a A_a$ . This motivates the definition,  $A_a = \frac{i}{\rho}(Y + Y_a)$ , where the factor of  $i$  is included for later convenience, and  $\sum_a Y_a = 0$ . Adding a Lagrange multiplier  $\frac{i}{\rho}\sum_a \text{STr}(Y_a\Lambda)$  to enforce the constraint, we are led to consider the functional  $\mathcal{Z}[j] = \int DY D\Lambda \exp(-S[Y, \Lambda])$ , with action

$$S[Y, \Lambda] = -\frac{1}{2\rho^2}\sum_a \text{STr}((Y + Y_a)P_a(Y + Y_a)) + \frac{i}{\rho}\sum_a \text{STr}(\Lambda Y_a) + \text{STr} \log(\hat{G}^{-1} + iwY),$$

where  $\rho = \binom{2N}{4}$  and we defined the operator  $\hat{P}_a B = \hat{X}_a B \hat{X}_a$ . Note that  $\hat{P}_a$  is self-inverse,  $\hat{P}_a^2 B = \hat{X}_a^2 B \hat{X}_a^2 = B$ , and hermitian in the sense that  $\text{STr}(C\hat{P}_a B) = \text{STr}(\hat{P}_a C B)$ . We now do the Gaussian integrals over  $Y_a$  to obtain,

$$S[Y, \Lambda] = -\text{STr}\left(\frac{\rho}{2}\Lambda\mathcal{P}\Lambda + i\Lambda Y\right) + \text{STr} \log(\hat{G}^{-1} + iwY),$$

where  $\mathcal{P} = \frac{1}{\rho}\sum_a \hat{P}_a$ . The Gaussian integration over  $\Lambda$  may now be performed and after rescaling  $Y \rightarrow \rho^{1/2}Y$ , and defining  $\gamma = w\rho^{1/2} = \frac{j}{2}(2N)^{1/2}$  we obtain the action  $S[Y] = -\frac{1}{2}\text{STr}(Y\mathcal{P}^{-1}Y) + \text{STr} \log\left(z - \hat{H}_2 + i\gamma Y\right)$ . In a final step, we perform a linear transformation  $\mathcal{P}^{-1}Y \rightarrow Y$ , and recall that in our units  $J^2 = 2/N$  and  $\gamma = 1$ , to arrive at Eq. (25).

### Appendix B: The operator $\mathcal{P}$

In this Appendix, we discuss the action of the operator  $\mathcal{P}$  states  $|n\rangle\langle n|$  diagonal in the occupation number basis. To this end, note that for a state  $|n\rangle =$

$|n_1, \dots, n_i, \dots, n_N\rangle$ , the action of the Majorana operator  $\hat{\chi}_{2i} = c_i + c_i^\dagger$  produces the state  $|n_i\rangle \equiv \hat{\chi}_{2i}|n\rangle = |n_1, \dots, \bar{n}_i, \dots, n_N\rangle$ , where  $\bar{n}$  is 0 for  $n = 1$ , and vice versa. Similarly,  $\hat{\chi}_{2i-1}|n\rangle = i(-)^{n_i}|n_i\rangle$ . Except for  $n_i$  all other occupation numbers remain unchanged, and no superpositions of states are generated. The adjoint action thus generates  $\hat{\chi}_{2i}|n\rangle\langle n|\hat{\chi}_{2i} = \hat{\chi}_{2i-1}|n\rangle\langle n|\hat{\chi}_{2i-1} = |n_i\rangle\langle n_i|$ , which we interpret as nearest neighbor hopping in Fock space. Notice that  $(\hat{\chi}_{2i}\hat{\chi}_{2i-1})|n\rangle\langle n|(\hat{\chi}_{2i-1}\hat{\chi}_{2i}) = |n\rangle\langle n|$  leaves the state unchanged.

With these structures in place, it is straightforward to describe the action of  $\mathcal{P}|n\rangle\langle n| = \frac{1}{\rho} \sum_a \hat{X}_a|n\rangle\langle n|\hat{X}_a$ . The summation contains contributions changing the particle number  $|n|$  by 0, 2 and 4. With  $\mathcal{P}_{n,m} = \langle m|(\mathcal{P}|n\rangle\langle n|)|m\rangle$ , the diagonal contribution,  $\mathcal{P}_0$  is obtained from the  $\binom{N}{2}$  terms of the structure  $\hat{\chi}_{2i}\hat{\chi}_{2i+1}\hat{\chi}_{2\beta}\hat{\chi}_{2\beta+1}$ . Similar counting for the contributions changing  $|n|$  by two and 4 gives the matrix elements stated in the main text,

$$\mathcal{P}_0 = \frac{N(N-1)}{2\rho}, \quad \mathcal{P}_2 = \frac{4(N-2)}{\rho}, \quad \mathcal{P}_4 = \frac{16}{\rho}, \quad (\text{B1})$$

and it is verified that

$$\begin{aligned} & \sum_m \mathcal{P}_{m,n} \\ &= \binom{N}{0} \frac{N(N-1)}{2\rho} + \binom{N}{2} \frac{4(N-2)}{\rho} + \binom{N}{4} \frac{16}{\rho} \\ &= 1. \end{aligned} \quad (\text{B2})$$

### Appendix C: Saddle point equations

In this Appendix we address the solution of the saddle point equation Eq. (5). The non-trivial element in this equation is the quantity  $\kappa_n \equiv \pi(\mathcal{P}\hat{\nu})_n$  in the denominator. In terms of this quantity, Eq. (5) becomes the simple algebraic equation (6). A closed yet site non-local equation for  $\kappa$  is obtained by acting on Eq. (5) with the operator  $\mathcal{P}$ ,

$$\begin{aligned} \kappa_n &= \sum_m \mathcal{P}_{|n-m|} \text{Im} \frac{1}{v_m - i\kappa_m} \\ &= \sum_m \mathcal{P}_{|n-m|} \text{Re} \int_0^\infty dt e^{iv_m t - \kappa_m t}, \end{aligned}$$

where in the second line switch to a temporal Fourier representation to facilitate the treatment of the argument  $v_m$ . The solution of this equation relies on two conceptual elements, first the ansatz Eq. (6) and second a replacement of the sum over the  $\rho$  neighboring sites  $m$  by a Gaussian average over energies  $v_m$ . Specifically, we note that up to corrections small in  $N^{-1}$ , the neighbor sites  $m$  are separated by Hamming distance 4 from  $n$  and each change in  $n_i$  changes  $v_n \mapsto v_n \pm 2v_i$ . This means that  $v_m = v_n + v$ , where we assume  $v$  to be Gaussian distributed with width  $\sqrt{4}\delta = 4\delta$ . Substituting the ansatz

$\kappa_m = \kappa\Theta(C - |v_m|)$  into the equation, and splitting the integral over  $v$  into regions with  $C - |v_m| = C - |v_n + v|$  smaller and larger than zero, respectively, we obtain after shifting  $v \mapsto v - v_n$

$$\begin{aligned} \kappa_n &= \frac{1}{\sqrt{32}\pi\delta} \text{Re} \int_0^\infty dt \\ &\times \left( \int dv e^{-\frac{(v-v_n)^2}{32\delta^2}} + \int_{-C}^C dv e^{-\frac{(v-v_n)^2}{32\delta^2}} (e^{-\kappa t} - 1) \right) e^{ivt}. \end{aligned}$$

With  $\text{Re} \int_0^\infty dt e^{ivt} = \pi\delta(v)$ , the first and the third term in the second line cancel out, and the  $t$ -integration of the second term gives

$$\kappa_n = \frac{\sqrt{\pi}}{\sqrt{32}\delta} \int_{-C}^C dv e^{-\frac{(v-v_n)^2}{32\delta^2}} \frac{\kappa}{\pi(v^2 + \kappa^2)}, \quad (\text{C1})$$

where the notation emphasizes that the  $\kappa$ -dependent term effectively represents a  $\delta_\kappa(v) = \frac{\kappa}{\pi(v^2 + \kappa^2)}$  in  $v$ , smeared over scales  $\sim \kappa$ . This expression defines the mean field amplitude  $\kappa_n$  at site  $n$  in dependence of the tolerance window  $C$  for the energy  $v_n$ , and  $\kappa$  itself. We now explore for which configurations  $(C, \kappa)$  it represents a self consistent solution.

The details of this analysis depend on whether we work with weakly (I, II) or strongly (III, IV) distributed on-site energies.

*Strong on-site disorder III, IV:* Anticipating that all solutions satisfy  $\kappa \ll 1$ , the width of  $\delta_\kappa(v)$  is much smaller than that of the Gaussian weight,  $\delta$ . The function  $\delta_\kappa$  thus collapses the integral, and we obtain

$$\kappa_n = \frac{\sqrt{\pi}}{\sqrt{32}\delta} e^{-\frac{v_n^2}{32\delta^2}}. \quad (\text{C2})$$

This is consistent with our ansatz with  $C = 2\delta$  and  $\kappa \sim \delta^{-1}$ .

*Narrow on-site disorder I, II:* In this regime, we test for the validity of the ansatz with  $C = 1$  and  $\kappa = 1$ . First assume  $|v_n| > 1 = C \gg \delta$ . In this case, the ansatz requires exponentially suppressed  $\kappa$ , the  $\delta_v$ -function again becomes effective, and the integral collapses to  $\kappa_n = \frac{\sqrt{\pi}}{\sqrt{32}\delta} \exp(-\frac{v_n^2}{32\delta^2})$  consistent with the assumed smallness of  $\kappa$ . Conversely, for  $|v_n| < 1 = C$ , the ansatz requires  $\kappa = 1$ . The function  $\delta_\kappa = \delta_1$  is now much wider than the width of the Gaussian,  $\sim \delta$ , and the integration boundaries can be extended to infinity. Doing the integral, we obtain  $\kappa_n \equiv \kappa = 1/\kappa$ , or  $\kappa = 1$ , consistent with Eq. (6).

### Appendix D: Effective matrix theory

In this appendix we discuss the derivation of Eqs. (36) and (37) from Eq. (25). In Eq. (25), we substitute  $Y \rightarrow \pi\hat{\nu}\hat{Q}$  with  $Q_n = T_n\sigma_3T_n^{-1}$ . The expansion of the action in fluctuations then comprises three parts: the Gaussian

weight, the expansion of the ‘Str log’ in site-to-site fluctuations, and the expansion of the ‘Str log’ in small frequency arguments,  $z$  (reflecting the non-commutativity,  $[z, T_n] \neq 0$ .)

*Gaussian weight:* A straightforward substitution yields

$$\begin{aligned} -\frac{1}{2}\text{STr}(Y\mathcal{P}Y) &\rightarrow -\frac{\pi^2}{2}\text{STr}(\hat{\nu}\hat{Q}\mathcal{P}(\hat{\nu}\hat{Q})) \\ &= -\frac{\pi^2}{2}\sum_{nm}\nu_n\nu_m P_{|n-m|}\text{STr}Q_nQ_m, \end{aligned} \quad (\text{D1})$$

where ‘STr’ includes the Fockspace trace, while ‘Str’ is only over internal degrees of freedom.

*Fluctuation action:* Substituting the ansatz into the ‘Str log’ and temporarily neglecting the frequency arguments,  $z$ , we obtain

$$\begin{aligned} &\text{STr}\log(-\hat{H}_2 + i\pi\mathcal{P}(\hat{\nu}\hat{Q})) \\ &= \text{STr}\log(-\hat{H}_2 + i\hat{T}^{-1}\pi\mathcal{P}(\hat{\nu}\hat{Q})\hat{T}) \\ &= \text{STr}\log(-\hat{H}_2 + i\pi\mathcal{P}(\hat{\nu}\sigma_3) + i\pi[\hat{T}^{-1}\mathcal{P}(\hat{\nu}\hat{Q})\hat{T} - \mathcal{P}(\hat{\nu}\sigma_3)]) \\ &\simeq \text{STr}\log(1 + \pi^2\hat{\nu}\sigma_3[\hat{T}^{-1}\mathcal{P}(\hat{\nu}\hat{Q})\hat{T} - \mathcal{P}(\hat{\nu}\sigma_3)]) \\ &\simeq \pi^2\text{STr}(\hat{\nu}\sigma_3[\hat{T}^{-1}\mathcal{P}(\hat{\nu}\hat{Q})\hat{T} - \mathcal{P}(\hat{\nu}\sigma_3)]) \\ &= \pi^2\text{STr}(\hat{\nu}\hat{Q}\mathcal{P}(\hat{\nu}\hat{Q})), \end{aligned} \quad (\text{D2})$$

identical to  $(-2\times)$  the Gaussian weight. In the second line we used the cyclic invariance  $\text{STr}\log(\dots)\text{STr}\log(\hat{T}^{-1}(\dots)\hat{T})$ , and in the fourth the saddle point equation  $(-\hat{H}_2 + i\pi\mathcal{P}(\hat{\nu}\sigma_3))^{-1} = -i\pi\hat{\nu}\sigma_3$ .

*Frequency action:* In a similar manner, we obtain

$$\begin{aligned} &\text{STr}\log(-\hat{H}_2 + i\pi\mathcal{P}(\hat{\nu}\hat{Q}) + z) \\ &\simeq \text{STr}\log(\hat{T}(-\hat{H}_2 + i\pi\mathcal{P}(\hat{\nu}\sigma_3))\hat{T}^{-1} + z) \\ &= \text{STr}\log(-\hat{H}_2 + i\pi\mathcal{P}(\hat{\nu}\sigma_3) + \hat{T}^{-1}z\hat{T}) \\ &\simeq -i\pi\text{STr}(\hat{\nu}\sigma_3\hat{T}^{-1}z\hat{T}) = -i\pi\text{STr}(\hat{\nu}\hat{Q}z), \end{aligned} \quad (\text{D3})$$

where in the first line, we neglected local fluctuations  $P(\hat{\nu}\hat{T}\sigma_3\hat{T}^{-1}) \simeq \hat{T}P(\hat{\nu}\sigma_3)\hat{T}^{-1}$ , in the third used cyclic invariance, and in the fourth the saddle point condition.

Combining terms, we obtain the effective action (36).

### Appendix E: Wave function and spectral statistics from matrix model

In this section we provide details on the computation of wave-function and spectral statistics in the deformed SYK<sub>4</sub> model. The starting point for both statistics is Eq. (32), with sources  $j = J_K$  or  $J = J_{I,n}$ , respectively, given in Eq. (19). Using the commutativity  $[T, \hat{H}_2] = 0$  we represent the action as

$$S[T] = \text{STr}\log\left(1 + \hat{G}\mathcal{O}_T\right) = \sum_{k=1}^{\infty}\frac{(-1)^k}{k}\text{STr}(\hat{G}\mathcal{O}_T)^k,$$

where  $\mathcal{O}_T \equiv T^{-1}[z - j(\alpha, \beta)]T$  is an operator in which we need to expand to the order required by the correlation function, and we have made the source contribution,  $j(\alpha, \beta)$ , to the matrix  $z = \frac{\omega+i\eta}{2}\sigma_3$  explicit again. Concerning the resolvent,  $\hat{G}^{-1} \equiv i\hat{\kappa}\sigma_3 - \hat{H}_2$ , we notice that fluctuation variables commute through the real part of  $\hat{G}$ , and keep only  $i\text{Im}\hat{G} = -i\pi\hat{\nu}$ , with local components  $\nu_n$  defined in Eq. (6). Specifically, to zeroth order in the sources, and first order in an expansion in  $z\nu_n \sim \omega/\Delta$ , the action assumes the form (33).

For the computation of the spectral and wave function statistics, we need the expansion in sources to first order in  $\beta$  and higher orders in  $\alpha$ . With the above definitions, the expansion of the action assumes the form

$$S[T] = -\pi\sum_{k=1}^{\infty}(-i\nu_n\alpha)^k\left(\frac{1}{k}[Q_{\text{bb}}^{++}]^k + \frac{\beta}{\alpha}[Q_{\text{bb}}^{++}]^{k-1}Q_{\text{ff}}^{--}\right), \quad (\text{E1})$$

where in the terms  $k > 2$  we used the approximation  $Q_{\text{bf}}^{+-}Q_{\text{fb}}^{-+} \simeq Q_{\text{bb}}^{++}Q_{\text{ff}}^{--}$  valid in the limit  $\eta \rightarrow 0$  implied in the calculation of wave function moments [35]. Doing the derivatives in the source parameters, we arrive at

$$\partial_{\alpha}^q\partial_{\beta}\mathcal{Z}|_{\alpha,\beta=0} = (-i\pi\nu_n)^q q! \langle [Q_{\text{bb}}^{++}]^{q-1}Q_{\text{ff}}^{--} \rangle, \quad (\text{E2})$$

where  $\langle \dots \rangle = \int dQ e^{-S_z[Q]}(\dots)$ .

The remaining integral over the four-dimensional matrix  $Q$  is conceptually straightforward but technically the hardest part of the calculation. Referring for details to Ref. 35, we here review the main steps. The starting point is a ‘polar coordinate’ representation  $Q = UQ_0U^{-1}$  with  $Q_0$  defined in Eq. (34),  $\hat{\theta} = \text{diag}(i\hat{\theta}_b, \hat{\theta}_f)$  containing compact and non-compact angles  $0 < \theta_f < \pi$  and  $\theta_b > 0$ , respectively [35]. The matrix  $U$  is block-diagonal in causal space and contains four Grassmann variables  $\eta^{\pm}, \bar{\eta}^{\pm}$ , and two more commuting variables  $0 \leq \phi, \hat{\chi} < 2\pi$ . More specifically,  $U = \text{diag}(u_1u_2, v)_{\text{ra}}$ , where  $u_2 = \text{diag}(e^{i\phi}, e^{i\hat{\chi}})_{\text{bf}}$  and supermatrices  $u_1 = e^{-2\hat{\eta}^+}$ ,  $v = e^{-2i\hat{\eta}^-}$ , generated by  $\hat{\eta}^{\pm} = \begin{pmatrix} 0 & \bar{\eta}^{\pm} \\ -\eta^{\pm} & 0 \end{pmatrix}_{\text{bf}}$ . In this representation, the matrix elements entering the correlation function are given by  $Q_{\text{bb}}^{++} = \cosh\theta_b(1 - 4\bar{\eta}^+\eta^+)$  and  $Q_{\text{ff}}^{--} = \cos\theta_f(1 - 4\bar{\eta}^-\eta^-)$ , and the integration measure reads  $dQ = \frac{1}{2^6\pi^2} \frac{\sinh\theta_b \sin\theta_f}{(\cosh\theta_b - \cos\theta_f)^2} d\phi d\hat{\chi} d\theta_b d\theta_f d\bar{\eta}^+ d\eta^+ d\bar{\eta}^- d\eta^-$  [35]. The essential advantage of the polar representation is that the action only depends on the ‘radial variables’  $S_{\eta}[Q] = -i2\pi\nu(\omega + i\eta)(\cosh\theta_b - \cos\theta_f)$ .

*Wave function statistics:* In the calculation of the wave function moments, we may set  $\omega = 0$ . The integration over the non-compact angle is then cut by the parameter  $\eta$  at values  $1 \leq \cosh\theta_b \lesssim 1/\eta$ , while the integration over the compact angles  $\theta_f$  is free. With this simplification, the integration over all variables except the non-compact

one,  $\theta$ , becomes elementary, and one obtains [35]

$$G_{nn}^{+(q-1)}G_{nn}^- = 2q(q-1)(-i\pi\nu_n)^q \times \int_0^\infty d\theta_b \sinh \theta_b (\cosh \theta_b)^{q-2} e^{-2\pi\nu\eta \cosh \theta_b}. \quad (\text{E3})$$

The final integral gives  $(2\pi\nu\eta)^{1-q}q!$  and collecting all factors we arrive at

$$I_q = \frac{q!}{\nu^q} \sum_n \nu_n^q. \quad (\text{E4})$$

This result expresses the  $n$ th moment of the local wave function amplitudes through that of the local density of states individually averaged over SYK<sub>4</sub> fluctuations. The energies  $v_n$  at each individual site are obtained as sums of  $N$  random coefficients  $v_i$  (cf. Eq. (3)). For large  $N$ , this makes the sum self averaging, and we replace  $I_q \rightarrow \langle I_q \rangle_\nu$  by its average over single particle energies,  $v_i$ . Using Eq. (6), we thus obtain

$$I_q = \frac{(-)^{q-1}q}{(\pi\nu)^q} \sum_n (\kappa_n)^q \left\langle \frac{\partial^{q-1}}{(\kappa_n)^2} \frac{1}{v_n^2 + (\kappa_n)^2} \right\rangle.$$

The evaluation of this expression now depends on which on-site disorder regime we are in. In regime I,  $\delta < N^{-1/2}$ , or  $|v_n| < 1$ , the mean field broadening assumes the uniform value  $\kappa = 1$ . In this case, the dependence of  $I_q$  on site energies,  $v_n$ , is weak. This implies  $\nu \simeq \frac{1}{\pi} \sum_n 1 = D/\pi$ . Doing the  $\kappa$  derivatives, we obtain

$$I_q = q!D^{1-q}, \quad \text{regime I}, \quad (\text{E5})$$

which is the RMT result for a matrix of dimension  $D$ .

For larger disorder, only a fraction of sites have finite decay width. Using Eq. (6) and assuming self averaging to replace the  $n$ -sum to an average over a distribution of site energies of width  $\delta N$ , the DoS is evaluated as

$$\begin{aligned} \nu &\simeq \frac{1}{\pi} \frac{D}{\sqrt{2\pi N\delta^2}} \int_{-C}^C dv e^{-\frac{v^2}{2N\delta^2}} \frac{\kappa}{v^2 + \kappa^2} \\ &\simeq \frac{1}{\pi} \frac{D}{\sqrt{2\pi N\delta^2}} \int_{-C}^C dv \frac{\kappa}{v^2 + \kappa^2} \\ &= \frac{1}{\pi} \frac{2D}{\sqrt{2\pi N\delta^2}} \arctan(C/\kappa), \end{aligned}$$

where in the second line we used that the distribution of energies is much wider than the tolerance window  $C$ . Substituting the values specified in Eq. (6), this leads to

$$\nu = c \frac{D}{\sqrt{N}\delta}, \quad (\text{E6})$$

where  $c$  is of order unity and the suppression relative to  $\nu = cD$  in regime I accounts for the improbability to find resonant sites.

In the same manner, we obtain

$$\begin{aligned} I_q &\simeq \frac{(-)^{q-1}q}{(\pi\nu)^q} \frac{D}{\sqrt{2\pi N\delta^2}} \kappa^q \partial_{\kappa^2}^{q-1} \int_{-C}^C dv e^{-\frac{v^2}{2N\delta^2}} \frac{1}{v^2 + \kappa^2} \\ &\simeq \frac{(-)^{q-1}q}{(\pi\nu)^q} \frac{D}{\sqrt{2\pi N\delta^2}} \kappa^q \partial_{\kappa^2}^{q-1} \int_{-C}^C dv \frac{1}{v^2 + \kappa^2} \\ &= 2 \frac{(-)^{q-1}q}{(\pi\nu)^q} \frac{D}{\sqrt{2\pi N\delta^2}} \kappa^q \partial_{\kappa^2}^{q-1} \frac{1}{\kappa} \arctan(C/\kappa) \\ &\simeq 2 \frac{(-)^{q-1}q}{(\pi\nu)^q} \frac{D}{\sqrt{2\pi N\delta^2}} \kappa^q \partial_{\kappa^2}^{q-1} \frac{1}{\kappa} \\ &= \frac{1}{(\pi\nu)^q} \frac{D}{\sqrt{2\pi N\delta^2}} \frac{2q(2q-3)!!}{(2\kappa)^{q-1}}, \end{aligned}$$

where ‘ $\simeq$ ’ here means equality up to some constant  $c \sim \mathcal{O}(1)$ . Insertion of Eq. (E6) leads to Eq. (13). Using Eq. (6), we finally obtain

$$q \gg 1: \quad I_q = c^q q! \left( \frac{D}{\sqrt{N}} \right)^{1-q} \begin{cases} \delta^{q-1}, & \text{II,} \\ \delta^{2(q-1)}, & \text{III.} \end{cases} \quad (\text{E7})$$

Finally, for a quantitative comparison to numerical simulations in regime III without fitting parameter we trace all constants  $c \sim \mathcal{O}(1)$  in  $\nu$  and  $I_q$ . Noting that in regime III we can substitute  $\arctan(C/\kappa) = \pi/2$  we arrive at,

$$I_q = \frac{q(2q-3)!!}{(2\pi\nu\kappa)^{q-1}} = \frac{q(2q-3)!!}{\delta^{2(1-q)}} \left( \frac{\pi D}{4\sqrt{N}} \right)^{1-q}, \quad \text{III} \quad (\text{E8})$$

where in the second equality we used Eq. (C2) for  $\kappa$ . *Level-statistics:* For the level statistics we need to keep finite  $\omega$ , and differentiate the functional to first order in  $\alpha$  and  $\beta$  (Eq. (21)). Application of Eq. (E2) then leads to [35]

$$\begin{aligned} K(\omega) &= \frac{1}{2} \text{Re} \int_0^\infty d\theta_b \int_{-\pi/2}^{\pi/2} d\theta_f \\ &\quad \times \sinh \theta_b \sin \theta_f e^{i\pi\nu\omega(\cosh \theta_b - \cos \theta_f)}, \quad (\text{E9}) \end{aligned}$$

where  $\theta_b$  and  $\theta_f$  are the non-compact bosonic and compact fermionic angle, respectively. These integrals can be carried out in closed form, and yield the two-point correlation function of the Gaussian Unitary Ensemble (9).

## Appendix F: Localization criterion

In this Appendix we demonstrate how the solution of the eigenvalue Equation (42) reduces to the criterion (43). We write the sum as

$$\begin{aligned} \Phi_n &= \frac{2\sqrt{\pi}}{\sqrt{\rho}} \sum_{|n-m|=4} a_{nm} \Phi_m, \\ a_{nm} &= \sqrt{\nu_n \nu_m} \log \left( \frac{\rho}{(2\pi)^2 \nu_n \nu_m} \right), \end{aligned}$$

and make the self consistent assumption that the sum over neighboring sites  $m$  is dominated by resonant sites, and that the solution,  $\Phi_n$ , too, are peaked at those sites. Under these conditions it makes sense to consider a zeroth order approximation  $a_{nm} \simeq a_{nm}^0 \equiv \sqrt{\nu_n \nu_m} 2 \log(\sqrt{\rho}/2\pi\nu_m)$ , neglecting site-to-site fluctuations of the logarithm. In a final step we will refine the result by perturbation theory in  $\delta a_{nm} \equiv a_{nm} - a_{nm}^0 = \sqrt{\nu_n \nu_m} \log(\nu_m/\nu_n)$ . Making the replacement  $a_{nm} \rightarrow a_{nm}^0$ , we observe that the equation is solved by  $\Phi_n \propto \sqrt{\nu_n}$ , provided that

$$1 = \frac{4\sqrt{\pi}}{\sqrt{\rho}} \sum_m \nu_m \log\left(\frac{\sqrt{\rho}}{2\pi\nu_m}\right), \quad (\text{F1})$$

where the sum extends over the  $Z \equiv \binom{N}{4}$  sites in Hamming distance 4 to  $n$  (i.e. the parameter  $Z$  defines the effective coordination number of the Fock space lattice.) We note that with the above eigenstates the first order perturbative correction to the unit eigenvalue Eq. (F1) is given by  $\langle \Phi | \delta \alpha | \Phi \rangle \propto \sum_{nm} \nu_n \nu_m \log(\nu_n/\nu_m) = 0$ , which we take as a self consistent justification to work with the zeroth order approximation. Turning to the consistency equation for the eigenvalue, we again replace the sum over nearest neighbors by an average over their distribution of energies (cf. a similar operation in Appendix C):

$$\sum_m \nu_m f(\nu_m) \simeq Z \langle \nu(v) f(\nu(v)) \rangle_v \simeq Z \frac{f\left(\frac{\sqrt{32}\delta}{\sqrt{\pi}}\right)}{\sqrt{32\pi}\delta},$$

$$\langle \dots \rangle_v = \frac{1}{\sqrt{2\pi}4\delta} \int dv e^{-\frac{v^2}{32\delta^2}} (\dots).$$

Here, the second equality is based on the observation that on the subset of active sites,  $v < \delta$ , where  $\nu(v)$  is non-vanishing, and  $\nu(v) = \frac{\pi}{\delta(v^2 + \delta^2)}$  becomes a  $\delta$ -function of width  $\sim \delta^{-1}$  and height  $\nu(0) = \pi/\kappa$  with  $\kappa = \frac{\sqrt{\pi}}{\sqrt{32}\delta}$  (cf. Eq. (C2)). The integral collapses to this resonance region, leading to the stated result. (Effectively, this is saying that only resonant sites contribute to the nearest neighbor sum.)

Application of this auxiliary identity to the eigenvalue equation Eq. (F1) leads to

$$1 = \frac{1}{\sqrt{2\rho}} \frac{Z}{\delta} \log\left(\sqrt{\frac{8\rho}{\pi}} \delta\right), \quad (\text{F2})$$

which is solved by

$$\delta_c = \frac{Z}{\sqrt{2\rho}} W(2Z\sqrt{\pi}), \quad (\text{F3})$$

with  $W$  the Lambert- $W$  function.

For  $N \gg 1$ , we may approximate  $Z = \binom{N}{4} \simeq N^4/24$  and  $\rho = \binom{2N}{4} \simeq (2N)^4/4!$ . The asymptotic expansion for large arguments,  $W(x) \simeq \ln(x) + \dots$  then leads to the estimate Eq. (43) in the main text.

- 
- [1] P. W. Anderson, *Absence of Diffusion in Certain Random Lattices*, Phys. Rev. **109**, 1492 (1958).
- [2] B. L. Altshuler, Y. Gefen, A. Kamenev, and L. S. Levitov, *Quasiparticle Lifetime in a Finite System: A Nonperturbative Approach*, Phys. Rev. Lett. **78**, 2803 (1997).
- [3] P. G. Silvestrov, *Decay of a Quasiparticle in a Quantum Dot: The Role of Energy Resolution*, Phys. Rev. Lett. **79**, 3994 (1997).
- [4] P. G. Silvestrov, *Chaos thresholds in finite Fermi systems*, Phys. Rev. E **58**, 5629 (1998).
- [5] I. V. Gornyi, A. D. Mirlin, and D. G. Polyakov, *Many-body delocalization transition and relaxation in a quantum dot*, Phys. Rev. B **93**, 125419 (2016).
- [6] I. V. Gornyi, A. D. Mirlin, D. G. Polyakov, A. L. Burin, *Spectral diffusion and scaling of many-body delocalization transitions*, Annalen der Physik (Berlin) **529**, 1600360 (2017).
- [7] D. Basko, I. Aleiner, and B. Altshuler, *Metal-insulator transition in a weakly interacting many-electron system with localized single-particle states*, Ann. Phys. **321**, 1126 (2006).
- [8] I. V. Gornyi, A. D. Mirlin, and D. G. Polyakov, *Interacting Electrons in Disordered Wires: Anderson Localization and Low- $T$  Transport*, Phys. Rev. Lett. **95**, 206603 (2005).
- [9] J. Suntajs, J. Bonca, T. Prosen, and L. Vidmar, *Quantum chaos challenges many-body localization*, arXiv:1905.06345.
- [10] D. A. Abanin, *et al.*, *Distinguishing localization from chaos: challenges in finite-size systems*, arXiv:1911.04501.
- [11] R. K. Panda, A. Scardicchio, M. Schulz, S. R. Taylor, and M. Žnidarič, *Can we study the many-body localisation transition?*, Eur. Phys. Lett. **128**, 67003 (2020)
- [12] P. Sierant, D. Delande, and J. Zakrzewski, *Thouless Time Analysis of Anderson and Many-Body Localization Transitions*, Phys. Rev. Lett. **124**, 186601 (2020)
- [13] X. Leyronas, P. G. Silvestrov, and C. W. J. Beenakker, *Scaling at the Chaos Threshold for Interacting Electrons in a Quantum Dot*, Phys. Rev. Lett. **84** (2000).
- [14] A. De Luca, B. L. Altshuler, V. E. Kravtsov, and A. Scardicchio, *Anderson Localization on the Bethe Lattice: Nonergodicity of Extended States*, Phys. Rev. Lett. **113**, 046806 (2014).
- [15] V. E. Kravtsov, I. M. Khaymovich, E. Cuevas, and M. Amini, *A random matrix model with localization and ergodic transitions*, New Journal of Physics **17**, 122002 (2015).

- [16] B. L. Altshuler, E. Cuevas, L. B. Ioffe, and V. E. Kravtsov, *Nonergodic Phases in Strongly Disordered Random Regular Graphs*, Phys. Rev. Lett. **117**, 156601 (2016).
- [17] V. E. Kravtsov, B. L. Altshuler, and L. B. Ioffe, *Non-ergodic delocalized phase in Anderson model on Bethe lattice and regular graph*, Annals of Physics **389**, 148 (2018).
- [18] K. S. Tikhonov, and A. D. Mirlin, *Statistics of eigenstates near the localization transition on random regular graphs*, Phys. Rev. B **99**, 024202 (2019).
- [19] E. J. Torres-Herrera, and L. F. Santos, *Extended non-ergodic states in disordered manybody quantum systems*, Ann. Phys. **529**, 1600284 (2017).
- [20] L. Faoro, M. Feigel'man, and L. Ioffe, *Non-ergodic extended phase of the Quantum Random Energy model*, Ann. of Phys. **409**, 167916 (2019).
- [21] G. Biroli, A. C. Ribeiro-Teixeira, and M. Tarzia, *Difference between level statistics, ergodicity and localization transitions on the Bethe lattice*, arXiv:1211.7334.
- [22] G. Biroli, and M. Tarzia, *Delocalization and ergodicity of the Anderson model on Bethe lattices*, arXiv:1810.07545.
- [23] G. Biroli, and M. Tarzia, *Delocalized glassy dynamics and many-body localization*, Phys. Rev. B **96**, 201114 (2017).
- [24] A. De Luca, B. L. Altshuler, V. E. Kravtsov and A. Scardicchio., *Anderson Localization on the Bethe Lattice: Nonergodicity of Extended States*, Phys. Rev. Lett. **113**, 046806 (2014).
- [25] K. S. Tikhonov, and A. D. Mirlin, *Statistics of eigenstates near the localization transition on random regular graphs*, Phys. Rev. B **99**, 024202 (2019).
- [26] K. S. Tikhonov, and A. D. Mirlin, *Critical behavior at the localization transition on random regular graphs*, Phys. Rev. B **99**, 214202 (2019).
- [27] X. Y. Song, C. M. Jian, and L. Balents, *Strongly Correlated Metal Built from Sachdev-Ye-Kitaev Models*, Phys. Rev. Lett. **119**, 216601 (2017).
- [28] S. Banerjee and E. Altman, *Solvable model for a dynamical quantum phase transition from fast to slow scrambling*, Phys. Rev. B **95**, 134302 (2017).
- [29] R. A. Davison, W. Fu, A. Georges, Y. Gu, K. Jensen, and S. Sachdev, *Thermoelectric transport in disordered metals without quasiparticles: The Sachdev-Ye-Kitaev models and holography*, Phys. Rev. B **95**, 155131 (2017).
- [30] D. Chowdhury, Y. Werman, E. Berg, and T. Senthil, *Translationally Invariant Non-Fermi-Liquid Metals with Critical Fermi Surfaces: Solvable Models*, Phys. Rev. X **8**, 031024 (2018).
- [31] A. A. Patel, J. Mc Greevy, D. P. Arovas, and S. Sachdev, *Magnetotransport in a Model of a Disordered Strange Metal*, Phys. Rev. X **8**, 021049 (2018).
- [32] A. V. Lunkin, K. S. Tikhonov, and M. V. Feigel'man, *Sachdev-Ye-Kitaev Model with Quadratic Perturbations: The Route to a Non-Fermi Liquid*, Phys. Rev. Lett. **121**, 236601 (2018).
- [33] A. Altland, D. Bagrets, and A. Kamenev, *Sachdev-Ye-Kitaev Non-Fermi-Liquid Correlations in Nanoscopic Quantum Transport*, Phys. Rev. Lett. **123**, 226801 (2019).
- [34] F. Wegner, *The mobility edge problem: Continuous symmetry and a conjecture*, Z. Phys. B **35**, 207 (1979).
- [35] K. B. Efetov, *Supersymmetry in Disorder and Chaos* (Cambridge Univ. Press, 1999).
- [36] T. Micklitz, F. Monteiro, and A. Altland, *Nonergodic Extended States in the Sachdev-Ye-Kitaev Model*, Phys. Rev. Lett. **123**, 125701 (2019).
- [37] S. Sachdev and J. Ye, *Gapless spin-fluid ground state in a random quantum Heisenberg magnet*, Phys. Rev. Lett. **70**, 3339 (1993).
- [38] A. Kitaev, <http://online.kitp.ucsb.edu/online/entangled15/kitaev/> ... /kitaev2/ (Talks at KITP on April 7th and May 27th 2015).
- [39] A. M. García-García, B. Loureiro, A. Romero-Bermúdez, and M. Tezuka, *Chaotic-Integrable Transition in the Sachdev-Ye-Kitaev Model*, Phys. Rev. Lett. **120**, 241603 (2018).
- [40] A. R. Kolovsky and D. L. Shepelyansky, *Dynamical thermalization in isolated quantum dots and black holes*, Eur. Phys. Lett. **117**, 10003 (2017).
- [41] Recalling conservation of fermion parity, distances are four, two, or zero.
- [42] Although the eigenvalues  $\{\pm v_i\}$  of  $J_{ij}$  are correlated, their sums, i.e. the eigenvalues of  $\hat{H}_2$ , become uncorrelated for large  $N$ .
- [43] Here we ignore corrections of  $\mathcal{O}(\frac{1}{N})$ . However, for numerically accessible sizes it is important to keep in mind the full expressions for the SYK<sub>4</sub> band width  $w_4 = \sqrt{\frac{3}{2N^4} \binom{2N}{4}}$ . Then, in order to still have the SYK<sub>2</sub> band width  $w_4 = \Delta$ , we need to rescale  $J_2 = \delta(1 - \frac{5}{2N} + \frac{3}{2N^2})^{1/2}$ .
- [44] Notice that the inverse participation ratio here has not been normalized by its value at  $\delta = 0$ , as in our previous publication [36].
- [45] A. Pal and D. Huse, *Many-body localization phase transition*, Phys. Rev. B **82**, 174411 (2010).
- [46] V. Oganesyan and D. Huse, *Localization of interacting fermions at high temperature*, Phys. Rev. B **75**, 155111 (2007).
- [47] More specifically, we used  $\delta_c = \frac{\sqrt{\pi}Z}{2\sqrt{\rho}} \log(\frac{\sqrt{\pi}Z}{32\pi^2})$ .
- [48] K. Truong and A. Ossipov, *Eigenvectors under a generic perturbation: Non-perturbative results from the random matrix approach*, Eur. Phys. Lett **116**, 37002 (2016).
- [49] Unlike with low dimensional single particle problems, the effectively high dimension of Fock space implies non-universality of the Thouless energy. For example, non-zero mode corrections to the spectral form factor (the Fourier transform of the two-point correlation function in energy) and the form factor itself, respectively, become visible at different energy scales.
- [50] Y. Y. Atas, E. Bogomolny, O. Giraud, and G. Roux, *Distribution of the Ratio of Consecutive Level Spacings in Random Matrix Ensembles*, Phys. Rev. Lett. **110**, 084101 (2013).
- [51] M.R.Zirnbauer, *Anderson Localization and Nonlinear  $\sigma$  Model With Graded Symmetry*, Nucl. Phys. B [FS] **265**, 375 (1986)
- [52] We here neglect the parametrically smaller number of sites with  $|n - m| = 2$  connected to  $n$  by matrix elements changing the occupation of just two fermion orbitals.